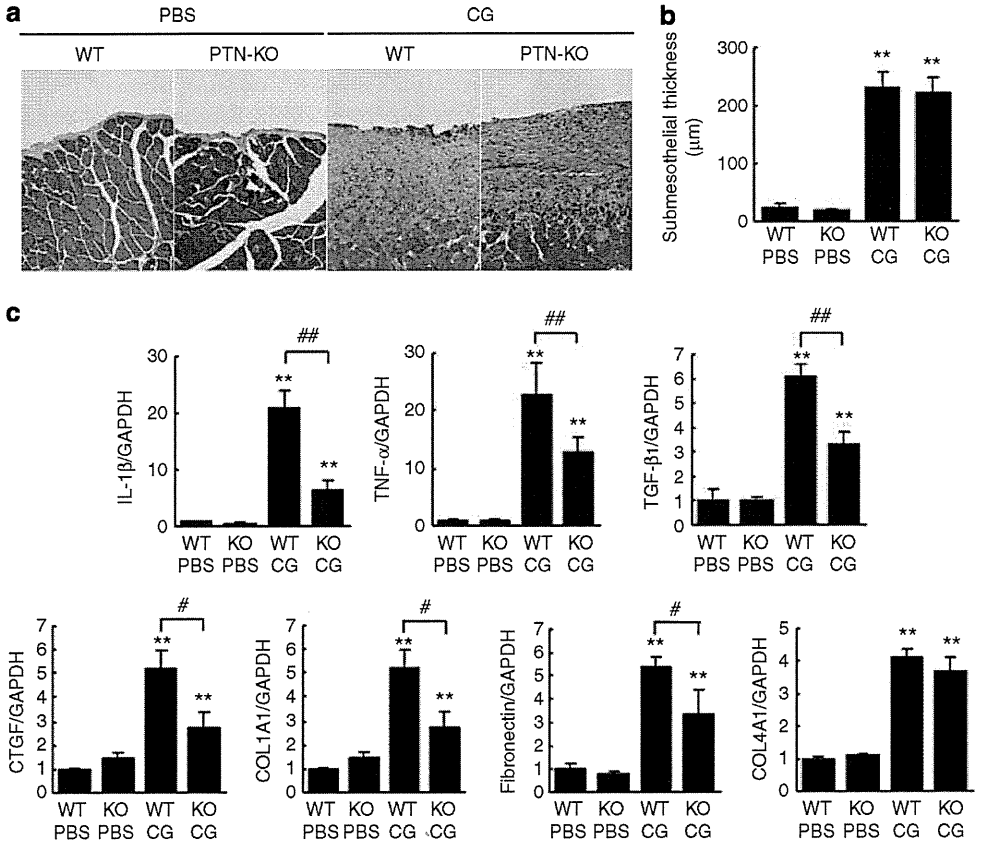

Figure 4 | Histological appearance and mRNA expression of peritoneum in PTN knockout mice (C57BL/6J background).[13] Pleiotrophin (PTN) knockout mice were treated with chlorhexidine gluconate (CG) three times a week for 4 weeks. (**a**) Masson's trichrome staining of peritoneum in wild-type or PTN knockout mice treated with phosphate-buffered saline (PBS) or CG. (**b**) The thickness of peritoneal membrane in mice. (**c**) Real-time reverse transcriptase-polymerase chain reaction analyses of interleukin (IL)-1β, tumor necrosis factor (TNF)-α, transforming growth factor (TGF)-β1, connective tissue growth factor (CTGF), fibronectin, α1(I) collagen (COL1A1), and a1(IV) collagen (COL4A1). GAPDH was used as control. WT PBS: $n=5$, KO PBS: $n=4$, WT CG: $n=11$, KO CG: $n=10$. Mean ± s.e. $^{**}P<0.01$ vs. PBS-treated mice with the same genotype. $^{\#}P<0.05$, $^{\#\#}P<0.01$. GAPDH, glyceraldehyde-3-phosphate dehydrogenase; KO, PTN knockout mice; WT, wild-type mice.

fibrin degradation products also correlate with increased peritoneal permeability.[22] IL-6 is an acute-phase inflammatory reaction protein. The dialysate and ascite levels of inflammatory and fibrinolysis markers have been reported to increase before the development of encapsulating peritoneal sclerosis.[23] Although levels of inflammatory, angiogenic, and fibrinolytic markers such as IL-6, vascular endothelial growth factor, and fibrin degradation products could be important biomarkers for developing encapsulating peritoneal sclerosis, key molecules involved in the process of peritoneal damage are still elusive. In this study, we performed microarray analysis to identify genes differentially expressed between PBS-treated and CG-treated mice and expressed in cultured mesothelial cells. *Procollagen type VIII α1* gene and IL-6 were upregulated by 73.5- and 25.9-fold, respectively. These genes have been already reported under peritoneal damage, indicating that our microarray analysis is consistent with previous reports.[4,24] Genes identified by microarray analysis can be candidate ones for elucidating the development and progression of peritoneal fibrosis. In this study, we detected increased PTN mRNA expression and protein levels by 42- and 4-fold, respectively. The discrepancy between mRNA and protein levels may come from long half-life of the protein.[25] Our study revealed that human peritoneal biopsy samples contained PTN mRNA and protein. PTN protein in human peritoneum was located at mesothelial cells and fibroblasts, consistent with mouse peritoneal fibrosis model. We also revealed that PTN was detected in overnight-dwell peritoneal dialysate and that the main form of PTN in peritoneal dialysate is 15 kDa. Previously, Lu *et al.*[14] have demonstrated that PTN15 promotes glioblastoma proliferation in an ALK-dependent manner, whereas PTN18 promotes migration in a Ptprz1-dependent manner. Peritoneal dialysates from patients with peritonitis may contain high levels of PTN.

PTN mRNA expression was increased in peritoneal fibrosis model mice mainly at fibroblasts. *In vitro* study also showed that PTN expression was abundant in cultured fibroblasts compared with cultured mesothelial cells, lymphocytes, and macrophages. PTN gene expression has been shown to be upregulated in NIH3T3 fibroblasts stimulated by

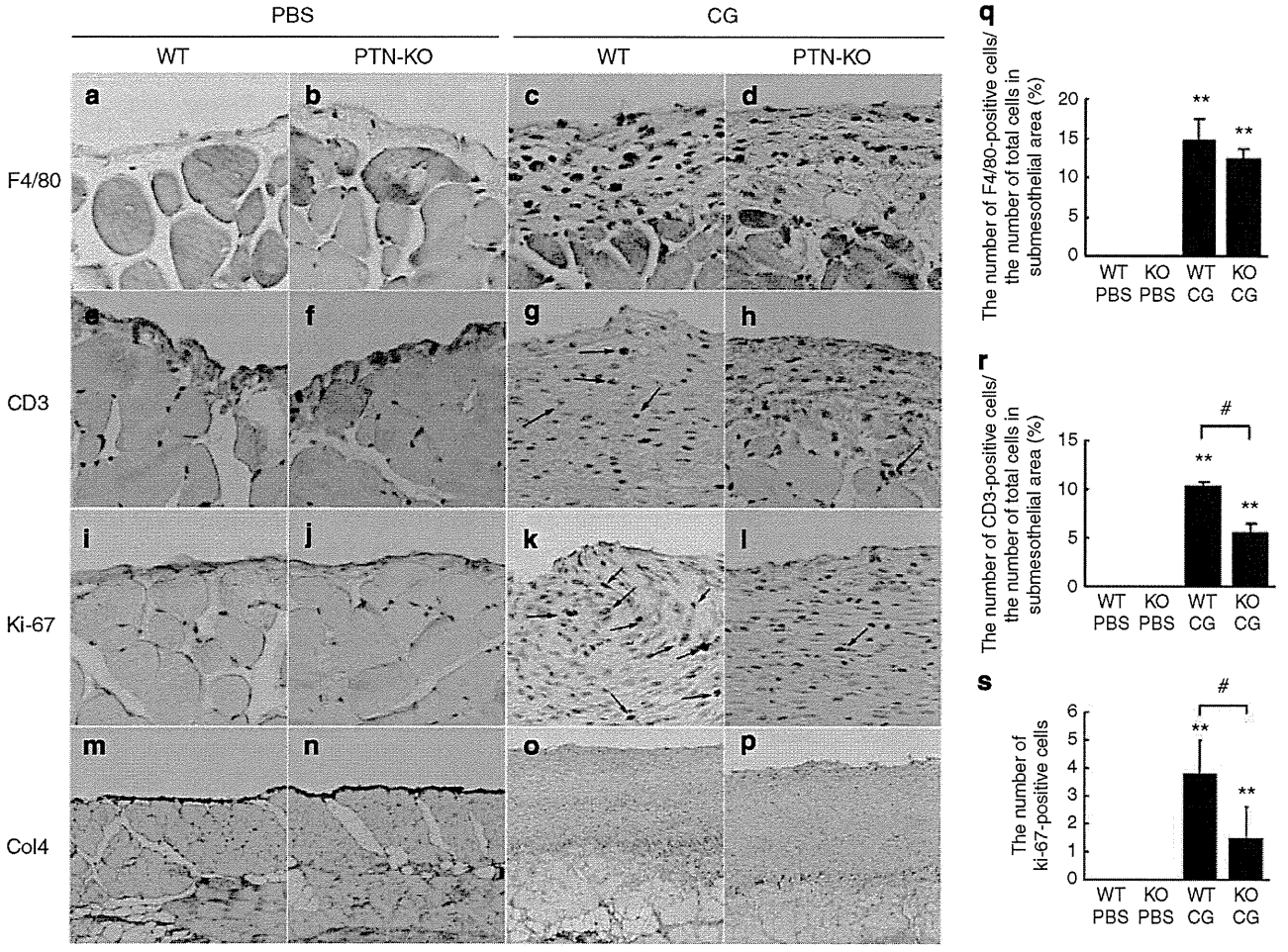

Figure 5 | Immunohistochemical study of F4/80, CD3, Ki-67, and type IV collagen (Col4). Mice were treated with chlorhexidine gluconate (CG) three times a week for 4 weeks. (**a–d**) F4/80, (**e–h**) CD3, (**i–l**) Ki67, and (**m–p**) Col4 staining in the peritoneum from (**a**, **e**, **i**, and **m**) phosphate-buffered saline (PBS)-injected wild-type (WT) mice, (**b**, **f**, **j**, and **n**) PBS-injected PTN knockout (KO) mice, (**c**, **g**, **k**, and **o**) CG-injected WT mice, (**d**, **h**, **l**, and **p**) CG-injected pleiotrophin (PTN)-KO mice. Arrows indicate positive cells. (**q**) The number of F4/80-positive cells per the number of total cells in the submesothelial area in mice. (**r**) The number of CD3-positive cells per the number of total cells in the submesothelial area in mice. (**s**) The number of Ki67-positive proliferated cells in the submesothelial area in mice. WT PBS: $n=5$, KO PBS: $n=4$, WT CG: $n=11$, KO CG: $n=10$. Mean ± s.e. $^{**}P<0.01$ vs. PBS-treated mice with the same genotype in Figure 5. $^{\#}P<0.05$.

platelet-derived growth factor-AB.[26] A recent paper reveals that PTN expression is strongly associated with IFN-γ/JAK/STAT1 signaling.[27] Further investigations are necessary to elucidate the molecular mechanism of PTN induction. PTN is a ligand of the RPTPβ/ζ,[12,28] ALK[12,] and syncecan-3.[12] Our study showed that RPTPβ/ζ was expressed in mesothelial cells, not in cultured fibroblasts, lymphocytes, or macrophages, and that syndecan-3 highly existed in mesothelial cells and was weakly expressed in fibroblasts and macrophages. ALK[29] was not detected in these cells. Taken together, PTN secreted by fibroblasts in submesothelial layer can have an effect on proliferation and migration mainly in mesothelial cells that express RPTPβ/ζ and syndecan-3.[30] The role of PTN receptors in peritoneal fibrosis needs further clarification.

In this study, the role of PTN in peritoneal fibrosis was investigated by using PTN-deficient mice. Without PTN, inflammatory and profibrotic responses were significantly reduced at 4 weeks after CG treatment, suggesting that PTN aggravates inflammation and fibrosis in the development of peritoneal fibrosis. Increased peritoneal permeability, examined by peritoneal equilibration tests, in CG-treated wild-type mice was almost completely ameliorated in CG-treated PTN knockout mice, suggesting that PTN can increase peritoneal permeability. Although CG-injected PTN knockout mice showed lower expression of COL1A1 and fibronectin than wild-type mice, the thickness of peritoneal membranes did not change between PTN-deficient mice and wild-type mice. The reason may come from similar expression levels of some other types of extracellular matrix such as collagen IV. Type IV collagen is abundantly deposited in peritoneal membrane.[31,32] Although macrophage infiltration has been shown to be an important phenomenon in peritoneal fibrosis,[33] CG-treated PTN-deficient mice showed no apparent difference in macrophage infiltration compared with wild-type mice. T cells are also an important part of

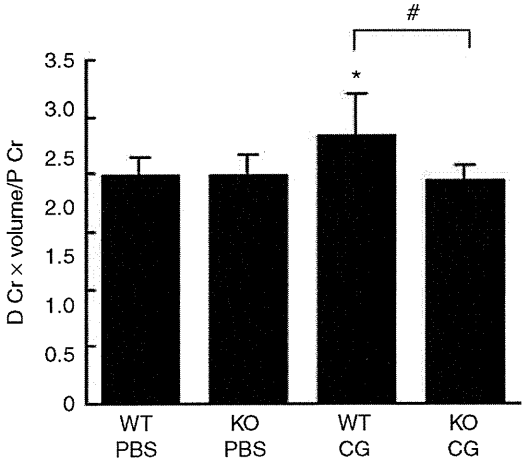

Figure 6 | Modified peritoneal equilibration test (PET). D Cr × volume/P Cr represents the creatinine (Cr) level of 7% glucose dialysate effluent (D) multiplied by volume divided by that of plasma (P) level in mice at 2 h retention. Chlorhexidine gluconate (CG)-injected wild-type (WT) mice showed increased D Cr × volume/P Cr compared with phosphate-buffered saline (PBS)-injected mice. Pleiotrophin (PTN)-knockout (KO) mice treated with CG showed reduced D Cr × volume/P Cr level compared with WT mice with CG. WT PBS: $n=3$, KO PBS: $n=6$, WT CG: $n=5$, KO CG: $n=7$. Mean ± s.e. $^{*}P<0.05$ vs. PBS-treated mice with the same genotype in Figure 6. $^{\#}P<0.05$.

peritoneal membrane damage,[34,35] and our results showed that T-cell infiltration was reduced in CG-treated PTN-deficient mice. PTN has been shown to induce expression of inflammatory cytokines in peripheral blood mononuclear cells.[36] The mechanism of T-cell infiltration by PTN is not clear, because RPTPβ/ζ mRNA nor syndecan-3 are not detected in cultured T-cell line. Downstream mediators of PTN need to be investigated in the future study. Cell proliferation was assessed by Ki-67 immunostaining.[37] PTN-deficient mice showed lower expression of Ki-67, indicating that cell proliferation in submesothelial layer was inhibited without PTN.

In conclusion, this study shows that PTN expression is upregulated in a mouse model of peritoneal fibrosis and is present in human peritoneal tissues and in peritoneal dialysate effluent, and that PTN secreted by fibroblasts or mesothelial cells can have a proliferative and chemotactic effect on mesothelial cells, and that PTN-deficient mice exhibit a weaker peritoneal membrane damage. These findings can be a help to elucidate a novel pathway in peritoneal fibrosis and suggest that PTN could be a promising biomarker against peritoneal damage.

MATERIALS AND METHODS

Patients

Patients who were admitted to Kyoto University Hospital for the diagnosis and treatment of renal disorders were enrolled under informed consent. This study was approved by the ethics committee on human research of Kyoto University Graduate School of Medicine. The parietal peritoneal samples were taken from the insertion site of a PD catheter located in the lumbar region as biopsies at the beginning or ending of PD. Peritoneal dialysate effluents were obtained at the time of the exchange. Expression of PTN in peritoneal biopsy sample was assessed by the RT-PCR method. After RNA extraction by RNeasy mini kit (Qiagen, Valencia, CA), complementary DNA was generated using the SuperScript II Reverse Transcriptase (Invitrogen, Carlsbad, CA) according to the manufacturer's instruction. RT-PCR was performed using the following primers: forward, 5′-gggaagaaagagaccagtgagt-3′ and reverse, 5′-ctggtttctctttcttccctgc-3′.

Induction of peritoneal fibrosis and phenotypic analysis

All animal experiments were approved by the animal experimentation committee of Kyoto University Graduate School of Medicine. Peritoneal fibrosis was induced in mice with the intraperitoneal injections of 0.3 ml of 0.1% CG in 15% ethanol and 85% PBS three times a week for 1, 2, 3, and 4 weeks as previously reported ($n=5$, each).[38] For evaluating dose–response, mice were administered 0.3 ml of 0.01% and 0.03% CG in 15% ethanol and 85% PBS three times a week for 4 weeks. Control mice received intraperitoneal injection of PBS. Mice were killed under pentobarbital anesthesia, and peritoneal tissues were obtained from the upper portion of the parietal peritoneum to avoid injured peritoneum by repeated injections.

For dialysis fluid infusion, silicone port catheters with two cuffs were used (PennyPort MMP-4S; Access Technologies, Skokie, IL). After mice were anesthetized under pentobarbital, an incision was made in the skin of the back and left lumbar portion. Peritoneal membrane was pricked with a 20-Gy needle to make a small hole. The catheter port was implanted under the skin of the back and the catheters were inserted along the needle hole. A catheter port was placed subcutaneously on the back. One milliliter of PDFs (Perisate; JMS, Hiroshima, Japan) containing 7% PD solution or PBS were administered intraperitoneally via a catheter port using a 26-Gy needle every day for 4 weeks ($n=5$, each). PTN-deficient mice (C57BL/6J background) were generated as described previously.[13]

Modified peritoneal equilibration test

Modified peritoneal equilibration test was conducted to determine the peritoneal permeability. Wild-type or PTN knockout mice were injected with PBS or CG ($n=5$, each) three times for 2 weeks, and were then administered intraperitoneal injection of 3 ml of 7% glucose dialysis solution (Perisate; JMS). After 2 h of retention, dialysis fluids were collected and blood samples were withdrawn. Serum and dialysate creatinine levels were measured by using the enzymatic method (SRL, Tokyo, Japan).

Affymetrix gene chip array

Wild-type mice were subjected to peritoneal fibrosis with the intraperitoneal injections of 0.3 ml of 0.1% CG in 15% ethanol and 85% PBS three times a week for 3 weeks ($n=3$). As control, PBS-treated wild-type mice were used ($n=3$). Total RNA from the parietal peritoneum at day 21 was extracted by RNeasy Mini Kit (Qiagen) in these mice.[39] Complementary RNA probes were generated using the GeneChip Expression 3′-Amplification Reagents for IVT Labeling Kit (Applied Biosystems, Foster city, CA) and each sample was hybridized to an Affymetrix mouse genome 430 2.0 array at TAKARA Bio (Shiga, Japan). After washing, the genechips were scanned by a GeneChip Scanner 3000. Data normalization, log transformation, statistical analysis, and pattern study were performed with the GeneChip Operating Software.

Histology and immunohistochemistry

Peritoneal membrane sections were fixed with 4% buffered paraformaldehyde and embedded in paraffin. Sections (1 μm thick) were stained with Masson's trichrome.[40] We measured the thickness of the fibrotic submesothelial zone above the abdominal muscle layer in cross-sections as described previously,[41] by using MetaMorph software (Molecular Devices, Downingtown, PA). Ten different points were examined by two investigators without knowledge of the origin of the slides. The results were expressed as the average peritoneal membrane thickness. For immunohistochemical analyses of PTN, collagen type IV, F4/80, CD3, and Ki-67 in mice, the sections were processed as described.[40] After antigen retrieval, the samples were incubated with rabbit polyclonal anti-PTN antibody (ProteinTech Group, Chicago, IL), rabbit polyclonal anti-mouse collagen type IV antibody (Millipore, Billerica, MA), rat monoclonal anti-F4/80 antibody (Serotec, Oxford, UK), rabbit polyclonal anti-CD3 antibody (DAKO, Glostrup, Denmark), and rat monoclonal anti-Ki-67 antibody (DAKO). After incubation with horseradish peroxidase-conjugated secondary antibodies, the specimens were developed using 3,3′-diaminobenzidine tetrahydrochloride. For immunohistochemical study of human PTN, we used a rabbit polyclonal anti-PTN antibody (Abcam, Cambridge, UK) as a primary antibody.

Real-time PCR analysis

Quantitative real-time PCR was performed using Premix Ex Taq (TAKARA Bio) on an Applied Biosystems 7300 real-time PCR system (Applied Biosystems) or a StepOnePlus system (Applied Biosystems), as described previously with some modification.[39] To determine mouse PTN, Ptprz1, TGF-β1, connective tissue growth factor, COL1A1, COL4A1, fibronectin, and IL-1β and tumor necrosis factor-α expression levels, gene-specific primers and probes were used. Primers and probe sequences are listed in Supplementary Table S1 online. Expression of each mRNA was normalized for glyceraldehyde-3-phosphate dehydrogenase using TaqMan Rodent glyceraldehyde-3-phosphate dehydrogenase control reagents (Applied Biosystems).

Western blot analysis

Western blot analysis was performed as described.[39] Filters transferred onto protein extracts or peritoneal dialysate effluents were incubated with rabbit polyclonal anti-PTN antibody (ProteinTech Group) and mouse monoclonal anti-glyceraldehyde-3-phosphate dehydrogenase antibody (Santa Cruz Biotechnology, Santa Cruz, CA). Immunoblots were then developed using a chemiluminescence kit (GE healthcare, Piscataway, NJ).

Cell culture

Mouse peritoneal mesothelial cells were obtained using a standard trypsin/ethylenediaminetetraacetic acid digestion method from the peritoneal wall of adult male C57BL/6J mice.[42,43] The excised peritoneal flap was cut into small pieces and then incubated, with constant agitation, with 0.25% trypsin and 1 mmol/l ethylenediaminetetraacetic acid (Invitrogen) for 15 min at 37 °C. The released cells were centrifuged at 1200 r.p.m. for 5 min and cultured with Dulbecco's Modified Eagle Medium (DMEM D6046; Sigma-Aldrich, St Louis, MI) supplemented with 10% fetal bovine serum (FBS), penicillin (100 U/ml), streptomycin (100 μg/ml), and amphotericin B (25 ng/ml). NIH3T3 fibroblasts, RAW264.7 cells, and bEnd.3 cells were obtained from American Type Culture Collection (Manassas, VA). BW5147 cells were provided by Health Science Research Bank (Sennan, Osaka, Japan) and BCL1-B20 cells were provided by the RIKEN BRC through the National Bio-Resource Project of the Ministry of Education, Culture, Sports, Science and Technology, Japan. BCL1-B20 cells were cultured with RPMI1640 (Sigma) with 10% FBS. Other cells were cultured with DMEM with 10% FBS.

Proliferation assay in cultured mesothelial cells was performed with ^{3}H-thymidine as described previously.[44] Briefly, mesothelial cells were plated on 24-well plates ($n = 6$, each group) and incubated with DMEM containing 0.3% FBS for the 24 h. Cell proliferation was studied in the presence of 1 ng/ml of recombinant human PTN (R&D Systems, Minneapolis, MN), 10 ng/ml of recombinant human platelet-derived growth factor-BB (BD Biosciences, San Jose, CA), 10^{-6} mol/l of angiotensin II (Peptide Institute, Osaka, Japan), 100 ng/ml of recombinant human endothelial growth factor (PeproTech EC, London, UK), or vehicle (PBS) for 24 h with DMEM containing 0.3% FBS. ^{3}H-thymidine was added simultaneously with the above-described agents. Migration assay was performed as described previously.[45] In brief, migration of mesothelial cells was analyzed by modified Boyden chamber method using 96-well chemotaxis chambers. In the upper chambers, mesothelial cells were placed with DMEM containing 0.02% bovine serum albumin. In the lower chambers, there were serum-free DMEM containing PTN (1 ng/ml), platelet-derived growth factor-BB (50 ng/ml), angiotensin II (10^{-6} mol/l), or endothelial growth factor (100 ng/ml). The cells were incubated for 4 h and the filters were stained with 0.5% Coomassie Brilliant Blue R250 (Nacalai Tesque, Kyoto, Japan) in 50% methanol, 40% water, and 10% acetic acid ($n = 6$, each).

Statistical analysis

Data are expressed as the mean ± s.e. Statistical analysis was performed using one-way analysis of variance as appropriate. A P-value < 0.05 was considered statistically significant.

DISCLOSURE

All the authors declared no competing interests.

ACKNOWLEDGMENTS

We gratefully acknowledge M Fujimoto and Y Sakashita and other lab members for technical assistance, and A Yamamoto for secretarial assistance. This work was supported in part by research grants from the Japanese Ministry of Education, Culture, Sports, Science and Technology, the Japanese Ministry of Health, Labour and Welfare, and Japan Baxter PD Fund.

SUPPLEMENTARY MATERIAL

Table S1. TaqMan primers and probe sequences.

Supplementary material is linked to the online version of the paper at http://www.nature.com/ki

REFERENCES

1. Ledebo I, Ronco C. The best dialysis therapy? Results from an international survey among nephrology professionals. *NDT Plus* 2008; **1**: 403–408.
2. Saxena R. Pathogenesis and treatment of peritoneal membrane failure. *Pediatr Nephrol* 2008; **23**: 695–703.
3. Yung S, Chan TM. Preventing peritoneal fibrosis—insights from the laboratory. *Perit Dial Int* 2003; **23**(S2): S37–S41.
4. Pecoits-Filho R, Araujo MR, Lindholm B *et al.* Plasma and dialysate IL-6 and VEGF concentrations are associated with high peritoneal solute transport rate. *Nephrol Dial Transplant* 2002; **17**: 1480–1486.
5. Lai KN, Lai KB, Szeto CC *et al.* Growth factors in continuous ambulatory peritoneal dialysis effluent. Their relation with peritoneal transport of small solutes. *Am J Nephrol* 1999; **19**: 416–422.

6. Oh KH, Jung JY, Yoon MO *et al.* Intra-peritoneal interleukin-6 system is a potent determinant of the baseline peritoneal solute transport in incident peritoneal dialysis patients. *Nephrol Dial Transplant* 2010; **25**: 1639–1646.
7. Margetts PJ, Kolb M, Galt T *et al.* Gene transfer of transforming growth factor-β1 to the rat peritoneum: effects on membrane function. *J Am Soc Nephrol* 2001; **12**: 2029–2039.
8. Margetts PJ, Kolb M, Yu L *et al.* Inflammatory cytokines, angiogenesis, and fibrosis in the rat peritoneum. *Am J Pathol* 2002; **160**: 2285–2294.
9. Aroeira LS, Aguilera A, Selgas R *et al.* Mesenchymal conversion of mesothelial cells as a mechanism responsible for high solute transport rate in peritoneal dialysis: role of vascular endothelial growth factor. *Am J Kidney Dis* 2005; **46**: 938–948.
10. Zakaria el R, Matheson PJ, Hurt RT *et al.* Chronic infusion of sterile peritoneal dialysis solution abrogates enhanced peritoneal gene expression responses to chronic peritoneal catheter presence. *Adv Perit Dial* 2008; **24**: 7–15.
11. Deuel TF, Zhang N, Yeh HJ *et al.* Pleiotrophin: a cytokine with diverse functions and a novel signaling pathway. *Arch Biochem Biophys* 2002; **397**: 162–171.
12. Jin L, Jianghai C, Juan L *et al.* Pleiotrophin and peripheral nerve injury. *Neurosurg Rev* 2009; **32**: 387–393.
13. Muramatsu H, Zou P, Kurosawa N *et al.* Female infertility in mice deficient in midkine and pleiotrophin, which form a distinct family of growth factors. *Genes Cells* 2006; **11**: 1405–1417.
14. Lu KV, Jong KA, Kim GY *et al.* Differential induction of glioblastoma migration and growth by two forms of pleiotrophin. *J Biol Chem* 2005; **280**: 26953–26964.
15. Milner PG, Li YS, Hoffman RM *et al.* A novel 17 kD heparin-binding growth factor (HBGF-8) in bovine uterus: purification and N-terminal amino acid sequence. *Biochem Biophys Res Commun* 1989; **165**: 1096–1103.
16. Rauvala H. An 18-kd heparin-binding protein of developing brain that is distinct from fibroblast growth factors. *EMBO J* 1989; **8**: 2933–2941.
17. Sakurai H, Bush KT, Nigam SK. Identification of pleiotrophin as a mesenchymal factor involved in ureteric bud branching morphogenesis. *Development* 2001; **128**: 3283–3293.
18. Amet LE, Lauri SE, Hienola A *et al.* Enhanced hippocampal long-term potentiation in mice lacking heparin-binding growth-associated molecule. *Mol Cell Neurosci* 2001; **17**: 1014–1024.
19. Ochiai K, Muramatsu H, Yamamoto S *et al.* The role of midkine and pleiotrophin in liver regeneration. *Liver Int* 2004; **24**: 484–491.
20. Yamamoto R, Nakayama M, Hasegawa T *et al.* High-transport membrane is a risk factor for encapsulating peritoneal sclerosis developing after long-term continuous ambulatory peritoneal dialysis treatment. *Adv Perit Dial* 2002; **18**: 131–134.
21. Kawanishi H, Moriishi M. Encapsulating peritoneal sclerosis: prevention and treatment. *Perit Dial Int* 2007; **27**(S2): S289–S292.
22. Kawanishi H, Fujimori A, Tsuchida K *et al.* Markers in peritoneal effluent for withdrawal from peritoneal dialysis: multicenter prospective study in Japan. *Adv Perit Dial* 2005; **21**: 134–138.
23. Kawanishi H, Harada Y, Noriyuki T *et al.* Treatment options for encapsulating peritoneal sclerosis based on progressive stage. *Adv Perit Dial* 2001; **17**: 200–204.
24. Xu X, Rivkind A, Pappo O *et al.* Role of mast cells and myofibroblasts in human peritoneal adhesion formation. *Ann Surg* 2002; **236**: 593–601.
25. Dreyfus J, Brunet-de Carvalho N, Duprez D *et al.* HB-GAM/pleiotrophin: localization of mRNA and protein in the chicken developing leg. *Int J Dev Biol* 1998; **42**: 189–198.
26. Li YS, Gurrieri M, Deuel TF. Pleiotrophin gene expression is highly restricted and is regulated by platelet-derived growth factor. *Biochem Biophys Res Commun* 1992; **184**: 427–432.
27. Li F, Tian F, Wang L *et al.* Pleiotrophin (PTN) is expressed in vascularized human atherosclerotic plaques: IFN-γ/JAK/STAT1 signaling is critical for the expression of PTN in macrophages. *FASEB J* 2010; **24**: 810–822.
28. Meng K, Rodriguez-Pena A, Dimitrov T *et al.* Pleiotrophin signals increased tyrosine phosphorylation of β-catenin through inactivation of the intrinsic catalytic activity of the receptor-type protein tyrosine phosphatase β/ζ. *Proc Natl Acad Sci U S A* 2000; **97**: 2603–2608.
29. Stoica GE, Kuo A, Aigner A *et al.* Identification of anaplastic lymphoma kinase as a receptor for the growth factor pleiotrophin. *J Biol Chem* 2001; **276**: 16772–16779.
30. Raulo E, Chernousov MA, Carey DJ *et al.* Isolation of a neuronal cell surface receptor of heparin binding growth-associated molecule (HB-GAM). Identification as N-syndecan (syndecan-3). *J Biol Chem* 1994; **269**: 12999–13004.
31. Mateijsen MA, van der Wal AC, Hendriks PM *et al.* Vascular and interstitial changes in the peritoneum of CAPD patients with peritoneal sclerosis. *Perit Dial Int* 1999; **19**: 517–525.
32. Saito H, Kitamoto M, Kato K *et al.* Tissue factor and factor V involvement in rat peritoneal fibrosis. *Perit Dial Int* 2009; **29**: 340–351.
33. Schilte MN, Celie JW, Wee PM *et al.* Factors contributing to peritoneal tissue remodeling in peritoneal dialysis. *Perit Dial Int* 2009; **29**: 605–617.
34. Glik A, Douvdevani A. T lymphocytes: the 'cellular' arm of acquired immunity in the peritoneum. *Perit Dial Int* 2006; **26**: 438–448.
35. Devuyst O, Margetts PJ, Topley N. The pathophysiology of the peritoneal membrane. *J Am Soc Nephrol* 2010; **21**: 1077–1085.
36. Achour A, M'Bika JB, Baudouin F *et al.* Pleiotrophin induces expression of inflammatory cytokines in peripheral blood mononuclear cells. *Biochimie* 2008; **90**: 1791–1795.
37. Endl E, Gerdes J. The Ki-67 Protein: Fascinating forms and an unknown function. *Exp Cell Res* 2000; **257**: 231–237.
38. Ishii Y, Sawada T, Shimizu A *et al.* An experimental sclerosing encapsulating peritonitis model in mice. *Nephrol Dial Transplant* 2001; **16**: 1262–1266.
39. Yokoi H, Mukoyama M, Mori K *et al.* Overexpression of connective tissue growth factor in podocytes worsens diabetic nephropathy in mice. *Kidney Int* 2008; **73**: 446–455.
40. Yokoi H, Mukoyama M, Nagae T *et al.* Reduction in connective tissue growth factor by antisense treatment ameliorates renal tubulointerstitial fibrosis. *J Am Soc Nephrol* 2004; **15**: 1430–1440.
41. Yoshio Y, Miyazaki M, Abe K *et al.* TNP-470, an angiogenesis inhibitor, suppresses the progression of peritoneal fibrosis in mouse experimental model. *Kidney Int* 2004; **66**: 1677–1685.
42. Tamura M, Osajima A, Nakayamada S *et al.* High glucose levels inhibit focal adhesion kinase-mediated wound healing of rat peritoneal mesothelial cells. *Kidney Int* 2003; **63**: 722–731.
43. Yung S, Li FK, Chan TM. Peritoneal mesothelial cell culture and biology. *Perit Dial Int* 2006; **26**: 162–173.
44. Suganami T, Mukoyama M, Sugawara A *et al.* Overexpression of brain natriuretic peptide in mice ameliorates immune-mediated renal injury. *J Am Soc Nephrol* 2001; **12**: 2652–2663.
45. Sawai K, Mori K, Mukoyama M *et al.* Angiogenic protein Cyr61 is expressed by podocytes in anti-Thy-1 glomerulonephritis. *J Am Soc Nephrol* 2003; **14**: 1154–1163.

ORIGINAL ARTICLE

The effect of glycosylation on plasma N-terminal proBNP-76 levels in patients with heart or renal failure

Toshio Nishikimi,[1,2] Masashi Ikeda,[3] Yosuke Takeda,[2] Toshihiko Ishimitsu,[2] Ikuko Shibasaki,[4] Hirotsugu Fukuda,[4] Hideyuki Kinoshita,[1] Yasuaki Nakagawa,[1] Koichiro Kuwahara,[1] Kazuwa Nakao[1]

See Editorial, p 95

[1]Department of Medicine and Clinical Science, Kyoto University Graduate School of Medicine, Kyoto, Japan
[2]Department of Hypertension and Cardiorenal Medicine, Dokkyo Medical University, Mibu, Tochigi, Japan
[3]Institute of International Education and Research, Dokkyo Medical University, Mibu, Tochigi, Japan
[4]Department of Cardiovascular Surgery, Dokkyo Medical University, Mibu, Tochigi, Japan

Correspondence to
Professor Toshio Nishikimi, Department of Medicine and Clinical Science, Kyoto University Graduate School of Medicine, 54, Shogoin-Kawara-cho, Sakyo-ku, Kyoto 606-8507, Japan; nishikim@kuhp.kyoto-u.ac.jp

Accepted 13 May 2011
Published Online First 30 June 2011

ABSTRACT

Objective Pro-brain natriuretic peptide (proBNP)-108 and N-terminal proBNP-76 (NT-BNP) contain seven sites for *O*-linked oligosaccharide attachment. Currently, levels of glycosylated NT-BNP are probably underestimated because it is not recognised by one antibody in the sandwich assay system. The pathophysiological significance of cardiac and plasma levels of non-glycosylated (nonglyNT-BNP) and glycosylated NT-BNP (glyNT-BNP) in heart failure (HF) and chronic renal failure (CRF) was investigated.

Methods Plasma samples from 186 patients with HF and 76 patients with CRF on haemodialysis were studied, together with 11 atrial tissue samples. To measure nonglyNT-BNP and glyNT-BNP, samples were incubated with or without deglycosylating enzymes and NT-BNP was measured using Roche Elecsys proBNP I. The percentage glyNT-BNP was calculated as glyNT-BNP/(glyNT-BNP + nonglyNT-BNP).

Results In HF, plasma BNP, nonglyNT-BNP and glyNT-BNP levels all increased with increasing disease severity (New York Heart Association class; $p<0.0001$), though the molar ratio remained constant (molar ratio, BNP:nonglyNT-BNP:glyNT-BNP = 1:2.4:9.6). Before haemodialysis for CRF, plasma BNP and nonglyNT-BNP were somewhat elevated, and glyNT-BNP was markedly increased (molar ratio, BNP:nonglyNT-BNP:glyNT-BNP = 1:8.5:82). After haemodialysis, plasma BNP, nonglyNT-BNP, atrial natriuretic protein and cGMP all declined ($p<0.0001$), but glyNT-BNP was unchanged. Notably, the percentage of glyNT-BNP was elevated before haemodialysis, and was further increased after haemodialysis ($p<0.0001$). Atrial tissue levels of BNP, nonglyNT-BNP and glyNT-BNP were similar.

Conclusion The findings suggest that most endogenous plasma NT-BNP is glycosylated and therefore undetectable with the current assay system, and that the relative glycosylation level is increased by haemodialysis.

INTRODUCTION

Brain natriuretic peptide (BNP; also termed B-type natriuretic peptide) is a cardiac hormone mainly produced and secreted by the ventricles. Ventricular wall stress and/or ischaemia stimulate expression of the BNP precursor proBNP-108,[1 2] which is thought to be cleaved to BNP-32 (BNP) and N-terminal proBNP-76 (NT-BNP) prior to its secretion.[3] Levels of both BNP and NT-BNP are elevated in heart failure (HF) and chronic renal failure (CRF); they are used for diagnosing and evaluating the severity of HF and CRF, and are predictive of patient prognosis.[4]

A recent study has shown that recombinant proBNP derived from mammalian cells has seven sites of *O*-linked oligosaccharide attachment within the N-terminal portion of the peptide.[5] Moreover, it was also shown that proBNP is a major form of immunoreactive BNP in the plasma of patients with severe HF; that most proBNP is glycosylated[6]; and that NT-BNP is also glycosylated in human plasma.[7] Elecsys proBNP I (Roche Diagnostics, Indianapolis, Indiana, USA) is an NT-BNP immunoassay that contains capture monoclonal and signal polyclonal antibodies that recognise NT-BNP [1–21] and NT-BNP[39–50], respectively. Notably, NT-BNP[39-50] contains glycosylation sites at amino acid residues 44 and 48, and a recent study demonstrated that *O*-linked oligosaccharide attachment almost completely inhibits the binding of the polyclonal signal antibody to the peptide (figure 1).[8 9] For that reason, Elecsys proBNP I is thought to measure only non-glycosylated NT-BNP (nonglyNT-BNP). However, neither the amount of glycosylated NT-BNP (glyNT-BNP) present in the plasma of patients with HF or CRF nor the clinical significance of glycosylation is known at present. We therefore measured plasma nonglyNT-BNP and glyNT-BNP levels in patients with HF and patients with CRF on haemodialysis, and considered the clinical significance of both molecular forms of NT-BNP. In addition, to investigate the molecular forms of NT-BNP in the heart before secretion, we also assessed their levels in human atrial tissue.

METHODS

Informed consent was obtained from each patient; the protocol was approved by the ethics committee of our institute and was carried out in accordance with the recommendations of the ethical committee of Dokkyo Medical University.

Study 1 (HF)

We enrolled 186 (108 men and 78 women; age range, 37–91 years; mean age, 67±10 years) Japanese patients with HF. The clinical characteristics of these patients are shown in table 1. The primary causes of HF were valvular heart disease (n=67), ischaemic heart disease (n=52), dilated cardiomyopathy (n=28) and others (n=39). At the time of

Heart 2012;**98**:152–161. doi:10.1136/heartjnl-2011-300102

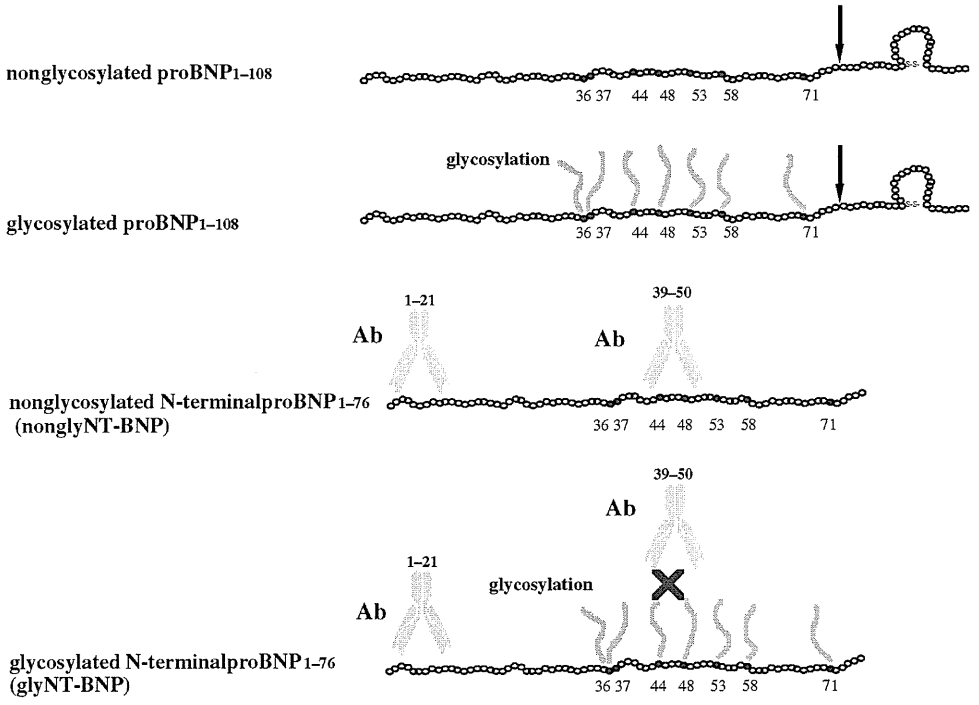

Figure 1 Schematic representation of nonglycosylated proBNP-108, glycosylated proBNP-108, nonglyNT-BNP and glyNT-BNP. proBNP1-108 can be post-translationally glycosylated at Thr36, Ser37, Ser44, Thr48, Ser53, Thr58 and/or Thr71 in its N-terminal region. ProBNP-108 and glycosylated proBNP-108 are cleaved to form the BNP-32 and nonglyNT-BNP or glyNT-BNP. Arrows indicate the cleavage site. The Roche NT-proBNP assay system uses two antibodies (Abs): a capture antibody targeting NT-proBNP amino acids 1–21 and a signal Ab recognising NT-proBNP amino acids 39–50. Glycosylation at Ser44 and Thr48 inhibits binding of the signal antibody. BNP, brain natriuretic protein; NT, N-terminal.

the study, the patients were being treated with angiotensin-converting enzyme inhibitors/angiotensin receptor blockers (72%), digitalis (38%) and/or diuretics (60%). The New York Heart Association (NYHA) functional classes were as follows: class I (n=82), mean age, 65±11 years; 50 men and 32 women; class II (n=82), 69±11 years; 46 men and 36 women; and class III–IV (n=22), 68±11 years; 12 men and 10 women. All groups had similar creatinine values. A patient with a creatinine value >2.5 mg/dl was excluded from the study.

Study 2 (CRF on haemodialysis)

We enrolled 76 (35 men and 41 women; age range, 32–84 years; mean age, 59±11 years) Japanese patients with end-stage renal failure who had been receiving haemodialysis for >6 months. All patients underwent regular haemodialysis for 3.5 h three times each week. The clinical characteristics of these patients are shown in table 2. The aetiologies of their CRF included chronic glomerulonephritis (n=35), diabetes mellitus (n=25), polycystic kidney disease (n=5), hydronephrosis (n=3), hypertensive nephrosclerosis (n=2) and unknown (n=6). These patients had a history of coronary artery disease (n=8), HF (n=6), vascular disease (n=5) and stroke (n=5). Cardiac function, heart size and blood pressure were relatively well controlled.

Table 1 Clinical characteristics of patients with heart failure in study 1

Variables	NYHA I	NYHA II	NYHA III–IV	p Value
Number	82	82	22	NS
Age (years)	65±11	69±11	68±11	NS
Gender (M/F)	50/32	46/36	12/10	NS
Aetiology				
IHD	14	30	8	NS
Cardiomyopathy	14	9	5	
Valvular heart	26	33	8	
Others	28	10	1	
Cre (mg/dl)	0.98±0.50	1.00±0.42	1.04±0.51	NS
LVEF (%)	61±9	54±15	39±8	<0.01
LVMI (g/m^2)	120±9	140±15	145±22	<0.01

Values are means±SD.
Cre, creatinine; F, female; IHD, ischaemic heart disease; LVEF, left ventricular ejection function; LVMI, left ventricular mass index; M, male; NS, non-significant; NYHA, New York Heart Association.

Study 3

In study 3, we assessed levels of BNP, nonglyNT-BNP and glyNT-BNP in atrial tissue from 11 other patients with HF who were in hospital to undergo cardiac surgery. The clinical characteristics of the patients who offered atrial tissue samples are presented in table 3. Resected samples of left atrial tissues from the 11 patients were frozen in liquid nitrogen and stored at −80°C.

Twelve volunteers with no obvious disease (6 male and 6 female; 50±10 years) served as healthy controls.

Table 2 Clinical characteristics of patients with chronic renal filure on haemodialysis in study 2

Variables	Means±SD
Age (years)	59±11
Gender (M/F)	35/41
Body height (m)	157±8
Body weight (kg)	48.7±8.8
Duration of haemodialysis (years)	14.2±5.7
Aetiology	
CGN	35 (46%)
Diabetes mellitus	25 (33%)
Other	16 (21%)
Haematocrit (%)	10.2±1.4
SBP (mm Hg)	139±20
DBP (mm Hg)	71±9
HR (beats/min)	72±8
Cardiothoracic ratio	49.6±4.0
LVEF (%)	65.5±8.8
FS (%)	35.9±6.6
LVMI (g/m^2)	98.0±23.3

Values are means±SD.
CGN, chronic glomerulonephritis; DBP, diastolic blood pressure; F, female; FS, fractional shortening; HR, heart rate; LVEF, left ventricular ejection fraction; LVMI, left ventricular mass index; M, male; SBP, systolic blood pressure.

Table 3 Clinical characteristics of patients with heart failure providing left atrial tissue

Variables	Atrial tissue
Number	11
Age (years)	65±9
Sex (female/male)	8/3
Operation	
MVR + maze	8
AVR + maze	1
CABG + maze	1
Atrial fibrillation	11
Duration <5 years	2
Duration ≥5 years	5
Duration unknown	4

Values are means±SD.
AVR, aortic valve replacement; CABG, coronary artery bypass graft; MVR, mitral valve replacement.

Blood sampling

Blood (3 ml) was withdrawn via the antecubital vein during study 1 to measure glyNT-BNP, nonglyNT-BNP and BNP, and via the shunt during study 2 before and after haemodialysis to measure glyNT-BNP, nonglyNT-BNP, BNP, atrial natriuretic peptide (ANP) and cGMP. Blood samples were transferred to chilled glass tubes containing disodium EDTA (1 mg/ml) and aprotinin (500 U/ml) and immediately centrifuged at 4°C, after which the plasma was frozen and stored at −80°C until used.

Assays of plasma ANP, BNP and cGMP levels

Plasma levels of BNP were measured using a fluorescent immunoenzyme assay (TOSO, Tokyo, Japan) as described previously.[10] Levels of ANP were measured using a specific immunoradiometric assay,[11] while levels of cGMP were measured using a radioimmunoassay,[12] as described previously.

Measurement of plasma glyNT-BNP and nonglyNT-BNP in HF and CRF

ProBNP-108 is post-translationally glycosylated to varying degrees at Thr36, Ser37, Ser44, Thr48, Ser53, Thr58 and Thr71 in its N-terminal region,[5] and NT-BNP is also glycosylated.[7] The Elecsys proBNP I is comprised of a capture monoclonal antibody that recognises NT-BNP[1–21] and a polyclonal signal antibody that recognises NT-BNP[39–50], which has glycosylation sites at amino acid residues 44 and 48 (figure 1).[9] Notably, *O*-linked oligosaccharide attachment almost completely inhibits the binding of the signal antibody to the peptide.[8 9] We therefore postulated that NT-BNP measured using Elecsys proBNP I is, in fact, nonglyNT-BNP. To measure total NT-BNP, 250 µl of plasma were diluted with 250 µl of 50 mM phosphate buffer (pH 6.0), after which portions of the diluted plasma (228 µl) were added to 12 µl of phosphate buffer, with or without a cocktail of deglycosylating enzymes, and incubated for 24 h at 37°C, as described.[5 7] The enzyme cocktail included *O*-glycosidase (Roche Diagnostics), neuraminidase (Roche Diagnostics), β-*N*-acetylglucosaminidase (Sigma, St Louis, Missouri, USA) and β-galactosidase (Sigma) at final concentrations of 6.25, 6.25, 62.5 and 625 mU/ml, respectively. *O*-Glycosidase and neuraminidase were essential for the deglycosylation, and the enzyme concentrations and incubation period were selected based on the results of preliminary and previously reported studies.[5 7] Our preliminary study showed that the enzyme reaction reaches a plateau under the conditions outlined above (figure 2A). The NT-BNP levels were then measured using Elecsys proBNP I, and the value obtained after deglycosylation

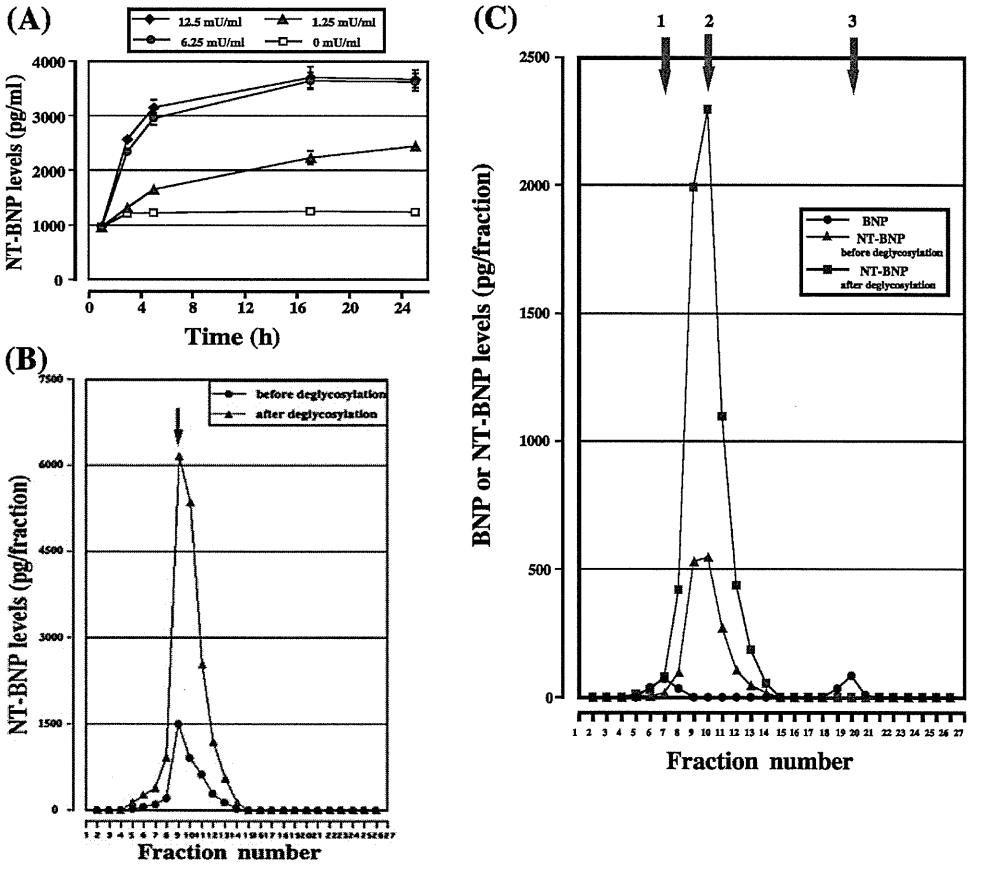

Figure 2 (A) Time course of N-terminal brain natriuretic peptide (NT-BNP) levels, with and without enzymatic deglycosylation. Diluted pooled plasma (n=10) was deglycosylated using 1.25, 6.25 or 12.5 mU/ml *O*-glycosidase and neuraminidase for 2, 4, 16 or 24 h. (B) Gel filtration high-performance liquid chromatography (HPLC) of NT-BNP from plasma extracts from patients with heart failure (HF), before and after deglycosylation, shows one peak corresponding to nonglyNT-BNP (arrow). (C) Gel filtration HPLC of NT-BNP and BNP from plasma extracts from patients with HF, before and after deglycosylation, shows three peaks corresponding to proBNP-108 (circles, left), nonglyNT-BNP (triangles and squares, centre) and BNP-32 (circles, right). Note that there is no NT-BNP peak corresponding to proBNP-108. A peak corresponding to NT-BNP increased after deglycosylation (squares, centre). Arrows: 1, proBNP-108; 2, nonglyNT-BNP; and 3, BNP-32.

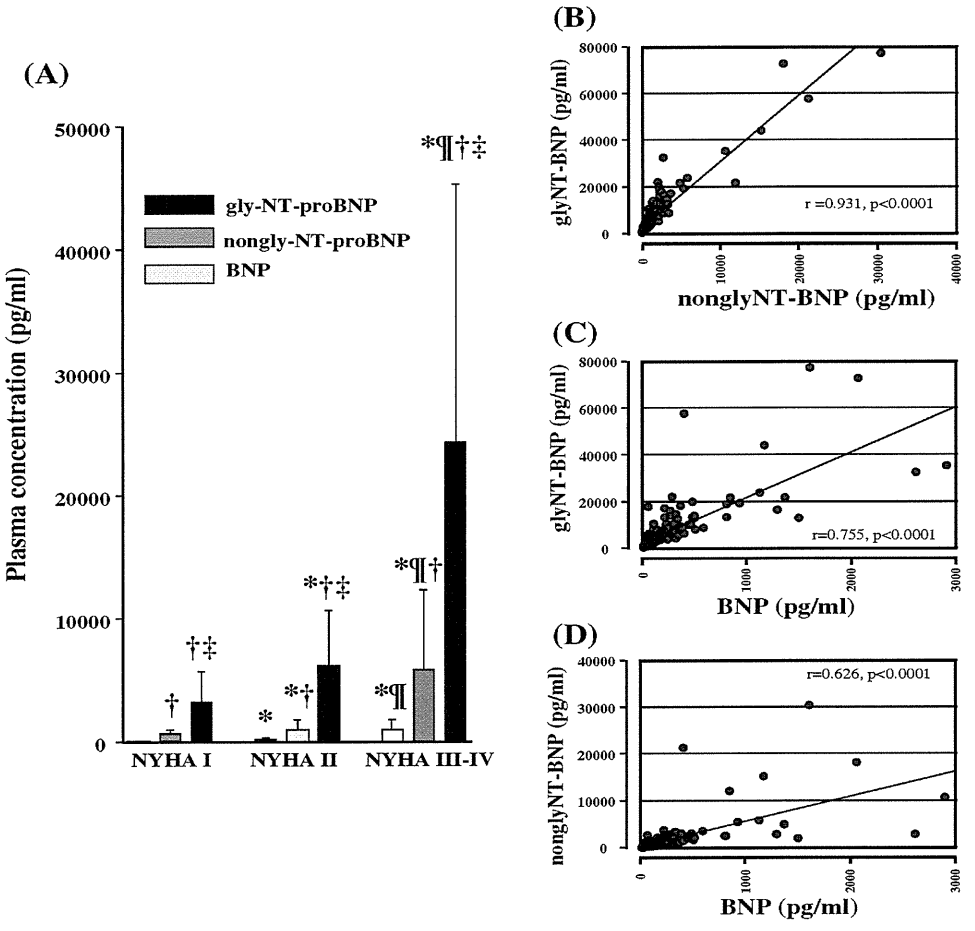

Figure 3 (A) Plasma levels of brain natriuretic peptide (BNP), non-glycosylated N-teminal BNP (nonglyNT-BNP) and glyNT-BNP in patients with heart failure (HF) in New York Heart Association (NYHA) functional classes I, II and III–IV. *p<0.01 vs NYHA class I; ¶p<0.01 vs NYHA class II; †p<0.01 vs BNP; ‡p<0.01 vs nonglyNT-BNP. (B–D) Relationships between plasma levels of glyNT-BNP and nonglyNT-BNP (B), nonglyNT-BNP and BNP (C), and glyNT-BNP and BNP (D) in patients with HF.

was postulated to be the total NT-BNP level. The glyNT-BNP was then calculated as total NT-BNP–nonglyNT-BNP, and the percentage glyNT-BNP was calculated as glyNT-BNP/(glyNT-BNP + nonglyNT-BNP) ×100%.

We also used a previously reported method[10] to determine the gel filtration profile of NT-BNP extracted from pooled plasma samples from patients with HF (n=10). In brief, we characterised the molecular forms of NT-BNP in peptide fractions extracted from human plasma using Sep-Pak C18 cartridge condensation. Gel filtration high-performance liquid chromatography (HPLC) was carried out using a TSK gel G2000SWXL column (TOSO). As shown in figure 2B, one peak with NT-BNP immunoreactivity and corresponding to the elution position of the recombinant nonglyNT-BNP (Hytest, Turku, Finland) was increased about fourfold after enzymatic deglycosylation. We also analysed the degree to which this NT-BNP assay system cross-reacted with proBNP using the same method. Using a fluorescence immunoassay system for BNP (TOSO), we measured NT-BNP and BNP immunoreactivity in the same

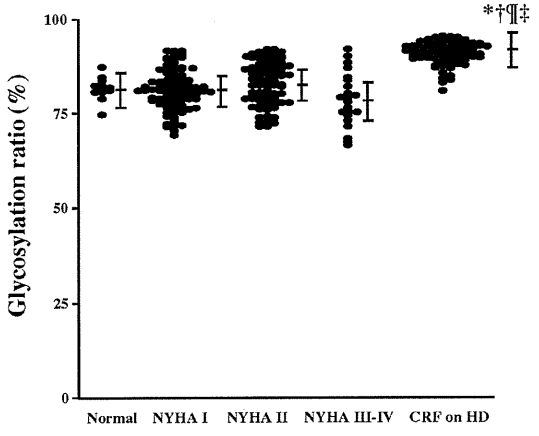

Figure 4 Percentage glycosylation in healthy individuals, patients with HF in New York Heart Association (NYHA) classes I, II and III–IV, and patients with chronic renal failure on haemodialysis. *p<0.01 vs healthy individuals; ¶p<0.01 vs NYHA class I; †p<0.01 vs NYHA class II; ‡p<0.01 vs NYHA class III–IV.

Table 4 Correlation coefficients and p values for patients with heart failure

Variables	Correlation coefficients	p Value
LVEF		
BNP	−0.406	<0.0001
GlyNT-BNP	−0.344	<0.0001
NonglyNT-BNP	−0.315	<0.0001
FS		
BNP	−0.329	<0.0001
GlyNT-BNP	−0.253	0.0045
NonglyNT-BNP	−0.226	0.0014
LVMI		
BNP	0.149	0.063
GlyNT-BNP	0.101	0.211
NonglyNT-BNP	0.147	0.061

BNP, brain natriuretic protein; FS, fractional shortening; LVEF, left ventricular ejection fraction; LVMI, left ventricular mass index; NT, N-terminal.

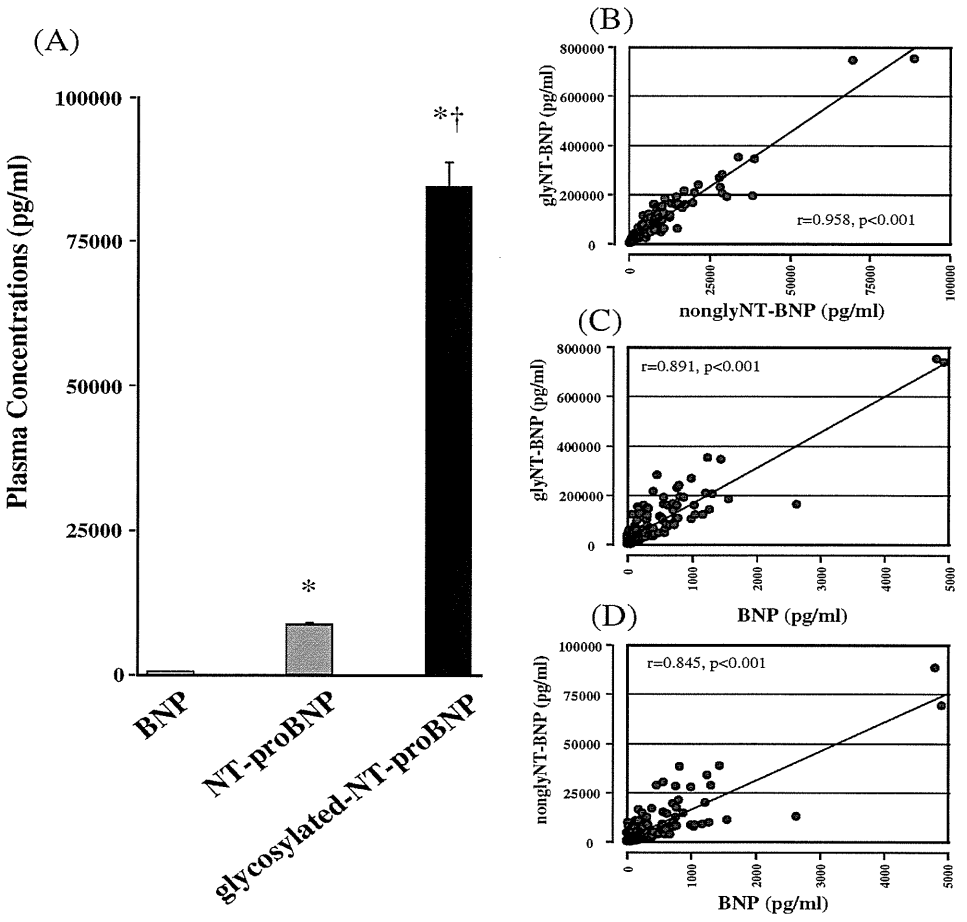

Figure 5 (A) Plasma levels of brain natriureic peptide (BNP), non-glycosylated N-terminal BNP (nonglyNT-BNP) and glyNT-BNP in patients with chronic renal failure (CRF) on haemodialysis. *p<0.01 vs BNP; †p<0.01 vs nonglyNT-BNP. (B–D) Relationships between plasma levels of glyNT-BNP and nonglyNT-BNP (B), glyNT-BNP and BNP (C) and nonglyNT-BNP and BNP (D) in patients with CRF on haemodialysis.

samples and obtained a single peak for NT-BNP (figure 2C, triangles), which was increased about fourfold after enzymatic deglycosylation (figure 2C, squares). In contrast, two peaks were obtained for immunoreactive BNP (figure 2C, circles): the first corresponded to proBNP-108, and the second to BNP-32. There was no obvious immunoreactive NT-BNP peak in the position corresponding to proBNP-108, indicating that the Elecsys assay system had little cross-reactivity with proBNP (<1%) (figure 2C). The deglycosylation procedure did not affect BNP levels.

Measurement of glyNT-BNP and nonglyNT-BNP in cardiac tissue

Samples of atrial tissue were boiled in 10 volumes of 1 mol/l acetic acid as described previously.[10] The tissue was then homogenised using a Polytron mixer and centrifuged, first at 3000 *g* and then at 15 000 *g*, for 15 min each at 4°C. The supernatant was extracted using a Sep-Pak C18 cartridge as described above for plasma. The eluate was lyophilised, dissolved in 30% acetonitrile containing 0.1% trifluoroacetic acid, and subjected to gel filtration HPLC on a TSK gel G2000SWXL column. Some fractions were subjected to the fluorescence immunoassay for BNP-32 and Elecsys II for NT-BNP in the same manner as the plasma samples. Others were dissolved in phosphate buffer; nonglyNT-BNP and glyNT-BNP were measured as described for plasma.

Echocardiographic measurements

In studies 1 and 2, an experienced echocardiographer without knowledge of the clinical features of the patients performed the echocardiographic study using a cardiac ultrasound unit (Sonos 5500; Philips Medical Systems, Andover, Massachusetts, USA).[13] Aortic diameter, left atrial diameter, interventricular thickness, posterior wall thickness, left ventricular end-diastolic diameter and left ventricular end-systolic diameter were all measured. Fractional shortening (FS), left ventricular mass index (LVMI) and left ventricular ejection fraction (LVEF) were calculated using standard formulae according to the recommendations of the American Society of Echocardiography.[14]

Statistical analysis

All values are expressed as means±SD. The statistical significance of differences between two groups was evaluated using the Fisher exact test or paired Student t test, as appropriate. The distribution of plasma peptide levels was normalised by log transformation, when appropriate. Variables were compared among three groups using one-way analysis of variance followed by the Bonferroni multiple comparison test. Correlation coefficients were calculated using linear regression analysis. Values of $p<0.05$ were considered significant.

RESULTS

Study 1

Plasma levels of BNP, nonglyNT-BNP and glyNT-BNP in patients with HF are shown in figure 3A. BNP was elevated to 106±72 pg/ml in NYHA class I (normal range <18.4 pg/ml), was increased to a significantly greater degree in NYHA class II, and was even higher in class III–IV. Levels of nonglyNT-BNP also increased with the HF severity, and were 5.6±4.3, 5.6±3.4 and 6.2±3.4 times higher than the BNP levels in NYHA classes I, II and III–IV, respectively. Similarly, levels of glyNT-BNP were increased to 34.7±27.7, 33.5±16.7 and 30.1±27.1 times higher than the BNP levels in the respective NYHA classes (figure 3A).

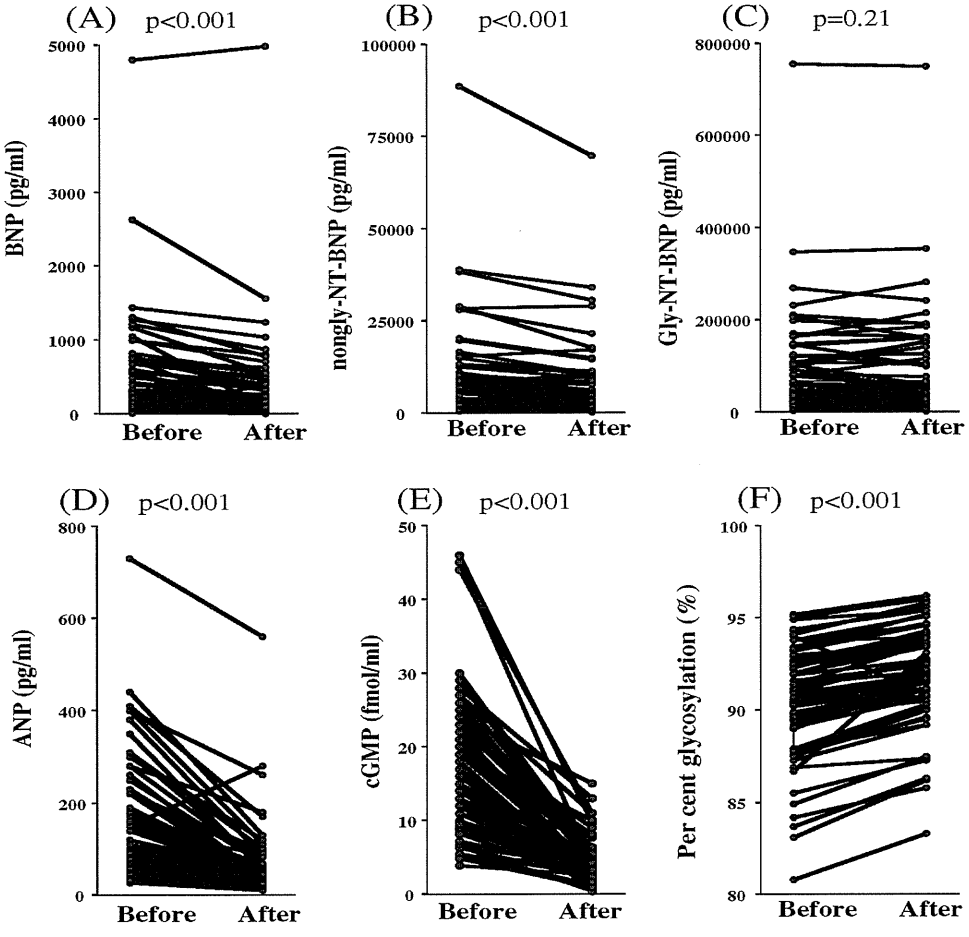

Figure 6 Plasma levels of brain natriureic peptide (BNP) (A), non-glycosylated N-terminal BNP (nonglyNT-BNP) (B), glyNT-BNP (C), atrial natriuretic peptide (ANP) (D), cGMP (E) and the percentage glycosylation (F) in patients with chronic renal failure before and after haemodialysis.

The percentage glycosylation in NYHA class I HF was 81±5%, suggesting that Elecsys proBNP I measures only ~20% of the total NT-BNP in this group of patients with HF. The percentage glycosylation did not differ significantly among the HF groups (figure 4), suggesting that glycosylation remains constant, irrespective of the severity of HF. On the other hand, the percentage glycosylation in patients with HF in any NYHA class was lower than in patients with CRF on haemodialysis (figure 4).

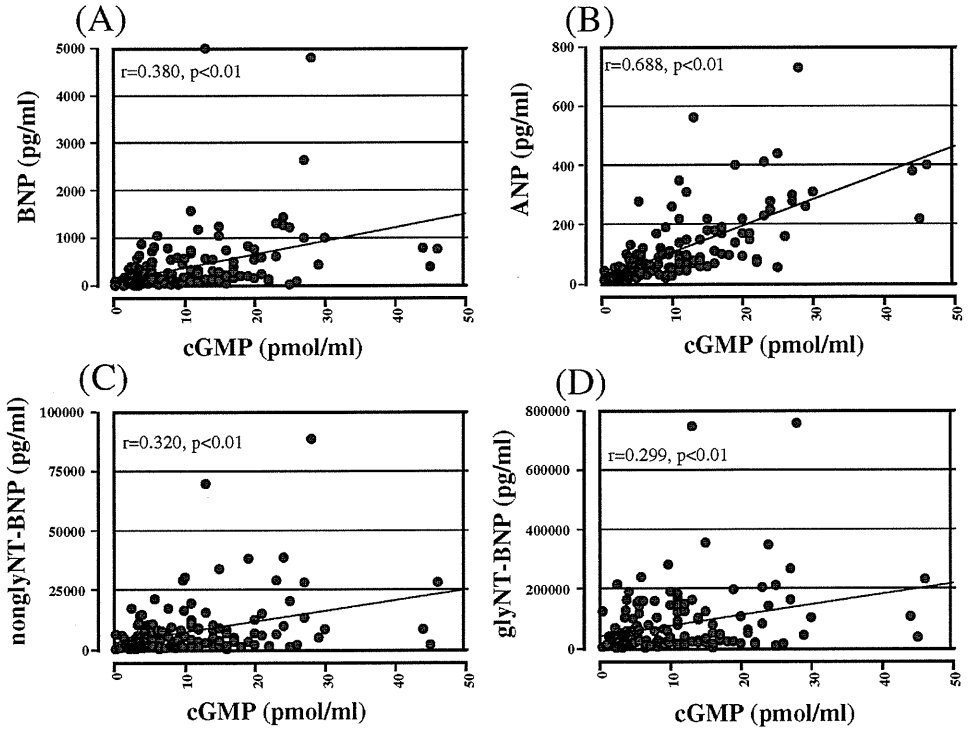

Figure 7 Relationships between plasma levels of cGMP and brain natriuretic peptide (BNP) (A), atrial natriuretic peptide (ANP) (B), non-glycosylated N-terminal BNP (nonglyNT-BNP) (C) and glyNT-BNP (D) in patients with chronic renal failure on haemodialysis.

Table 5 Correlation coefficients and p values for patients with chronic renal failure

Variables	Correlation coefficients	p Value
LVEF		
BNP	−0.557	<0.001
GlyNT-BNP	−0.499	<0.001
NonglyNT-BNP	−0.537	<0.001
FS		
BNP	−0.485	<0.001
GlyNT-BNP	−0.487	<0.001
NonglyNT-BNP	−0.509	<0.001
LVMI		
BNP	0.421	<0.001
GlyNT-BNP	0.522	<0.001
NonglyNT-BNP	0.520	<0.001

BNP, brain natriuretic protein; FS, fractional shortening; LVEF, left ventricular ejection fraction; LVMI, left ventricular mass index; NT, N-terminal.

Relationships between glyNT-BNP and ANP, BNP and nonglyNT-BNP

The relationships between glyNT-BNP and nonglyNT-BNP and BNP are shown in figure 3B,C. Plasma glyNT-BNP levels closely correlated with plasma nonglyNT-BNP and BNP in HF patients (nonglyNT-BNP, r=0.931; BNP, r=0.755; all p<0.0001). In addition, the nonglyNT-BNP and BNP levels were also significantly correlated (r=0.626, all p<0.0001, figure 3D).

Relationships of glyNT-BNP, nonglyNT-BNP and BNP with LVEF, FS and LVMI

The relationships of plasma levels of glyNT-BNP, nonglyNT-BNP and BNP with LVEF, FS and LVMI are shown in table 4. BNP, glyNT-BNP and nonglyNT-BNP levels significantly correlated with both LVEF and FS to similar degrees, but not with LVMI (table 4). In addition, the percentage glycosylation did not correlate with either the EF (r=0.06, NS) or creatinine (r=0.07, NS).

Study 2

Plasma concentrations of BNP, glyNT-BNP, nonglyNT-BNP, ANP and cGMP in CRF before and after haemodialysis

Plasma levels of BNP, nonglyNT-BNP and glyNT-BNP in patients with CRF before haemodialysis are shown in figure 5A. BNP was increased to 367±365 pg/ml (normal range <18.4 pg/ml), while nonglyNT-BNP was increased to 7455±8348 pg/ml, or ~20 times higher than the BNP level. glyNT-BNP was

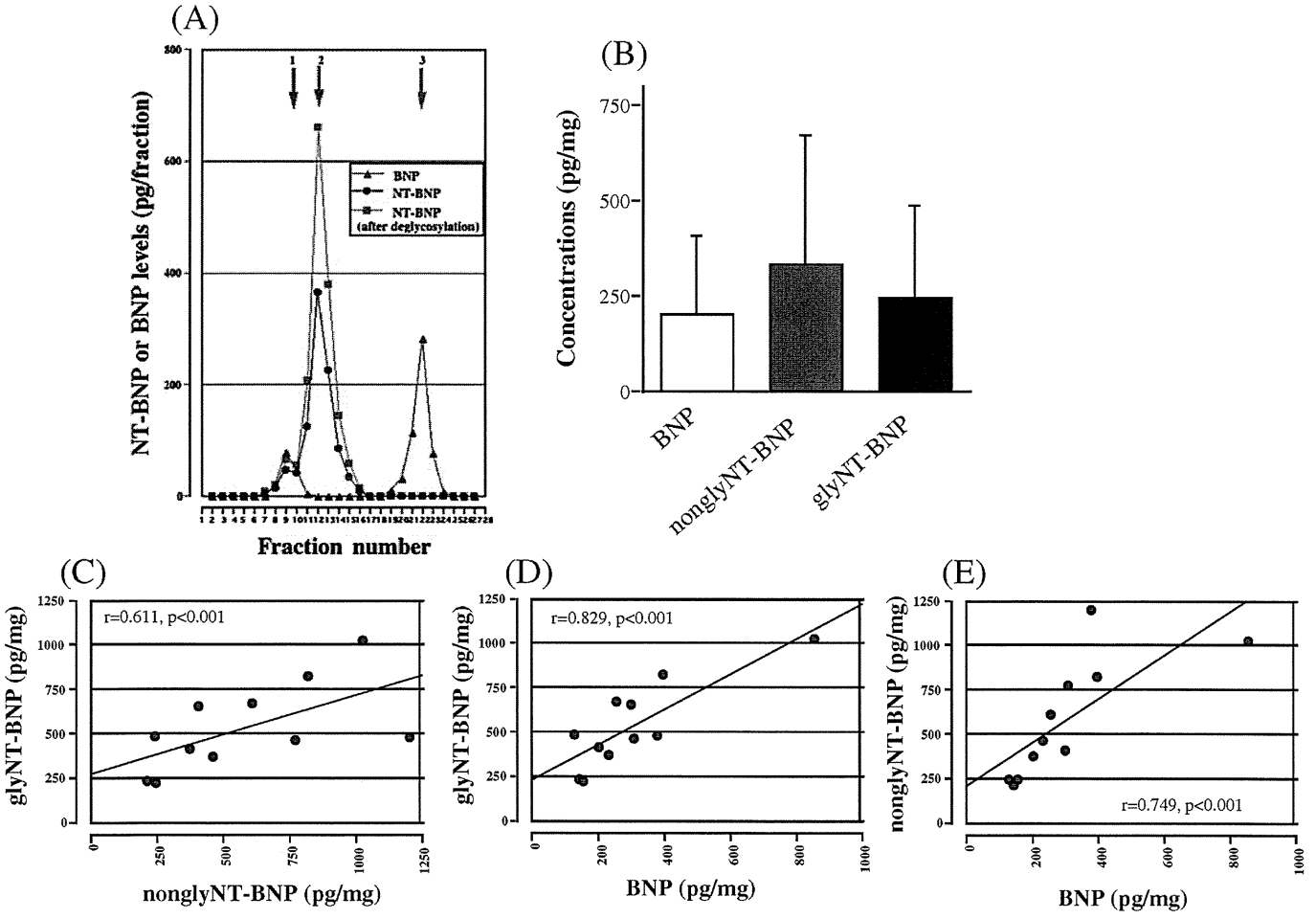

Figure 8 (A) Using tissue samples from patients with heart failure (HF), gel filtration high-performance liquid chromatography (HPLC) of N-terminal brain natriuretic peptide (NT-BNP) and BNP in atrial extracts before and after deglycosylation showed three peaks corresponding to proBNP-108 (circles, left), non-glycosylated NT-BNP (nonglyNT-BNP; triangles and squares, centre) and BNP-32 (circles, right). Note that there is a small peak corresponding to proBNP-108. The peak corresponding to NT-BNP increased after deglycosylation (squares, centre). Arrows: 1, proBNP-108; 2, nonglyNT-BNP; 3, BNP-32. (B) Atrial levels of BNP, nonglyNT-BNP and glyNT-BNP in patients with HF. (C–E) Relationships between atrial levels of glyNT-BNP and nonglyNT-BNP (C), glyNT-BNP and BNP (D), and nonglyNT-BNP and BNP (E) in patients with HF.

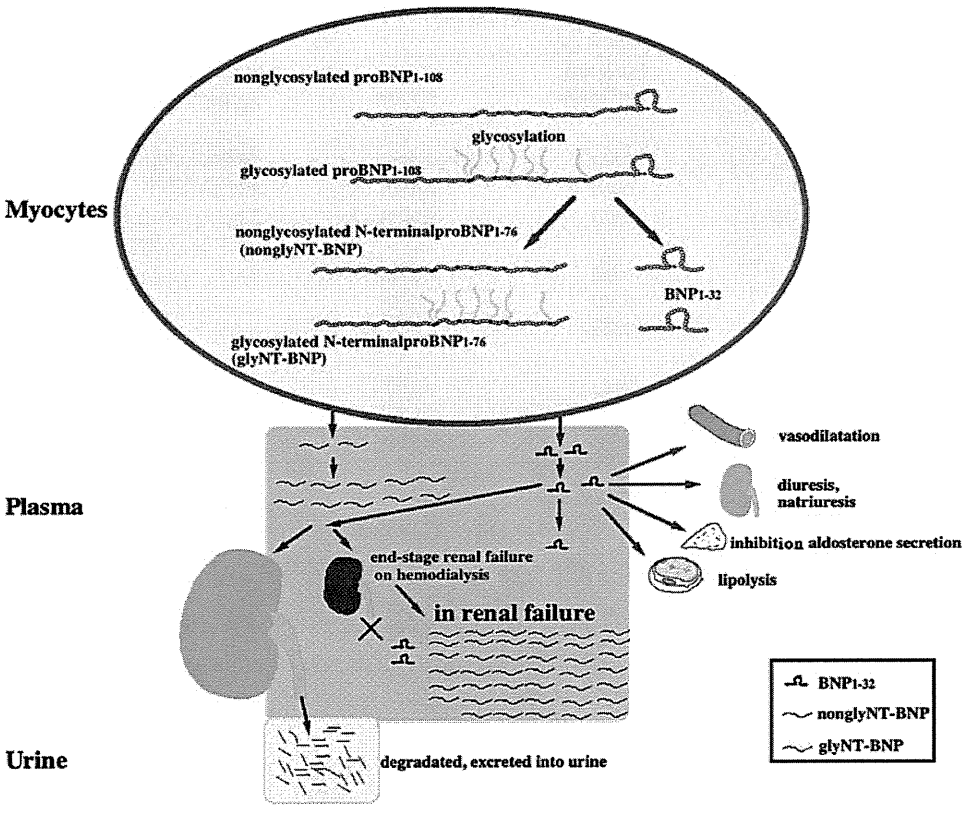

Figure 9 Schematic representation of a model of the production, secretion and metabolism of non-glycosylated N-terminal brain natriuretic peptide (nonglyNT-BNP), glyNT-BNP and BNP-32. Non-glycosylated proBNP-108 and glycosylated proBNP-108 are produced in myocytes and cleaved to nonglyNT-BNP, glyNT-BNP and BNP-32 by a processing enzyme prior to their secretion. BNP-32 binds to natriuretic receptor-A and exerts such effects as vasodilation, diuresis, natriuresis, inhibition of aldosterone secretion and lipolysis, among others. In contrast, nonglyNT-BNP and glyNT-BNP have no known physiological activity and are excreted mainly in the urine. In patients with chronic renal failure on haemodialysis, nonglyNT-BNP and glyNT-BNP are not excreted in the urine, and are therefore markedly elevated in the blood.

markedly increased to 69 122±69 554 pg/ml, or ~200 times higher than the BNP level and nine times higher than the nonglyNT-BNP level.

After haemodialysis, plasma levels of BNP, nonglyNT-BNP, ANP and cGMP were all significantly reduced ($p<0.0001$) (figure 6A–E), whereas levels of glyNT-BNP were unchanged ($p=0.21$) (figure 6F).

The percentage glycosylation before haemodialysis was 91.1±2.2% (figure 4), suggesting that only ~9% of total NT-BNP was detected using the Elecsys proBNP I assay system. Notably, the percentage glycosylation was significantly increased after haemodialysis ($p<0.0001$, figure 6F).

Relationships among glyNT-BNP, BNP and nonglyNT-BNP

The relationships among the plasma levels of glyNT-BNP, nonglyNT-BNP and BNP in patients with CRF on haemodialysis are shown in figure 5B–D. glyNT-BNP levels closely correlated with nonglyNT-BNP and BNP in patients with CRF (nonglyNT-BNP, $r=0.958$; BNP, $r=0.891$; all $p<0.0001$) (figure 5B,C). In addition, levels of nonglyNT-BNP and BNP were also significantly correlated ($r=0.845$, all $p<0.0001$, figure 5D).

Relationships between cGMP and glyNT-BNP, ANP, BNP and nonglyNT-BNP

Plasma levels of cGMP, a second messenger of ANP and BNP, significantly correlated with ANP and BNP levels and weakly correlated with levels of nonglyNT-BNP and glyNT-BNP (figure 7A–D).

Relationships of glyNT-BNP, nonglyNT-BNP and BNP with LVEF, FS and LVMI

Plasma BNP is a known marker of left ventricular function and hypertrophy, even in patients with CRF on haemodialysis. Consistent with that, we found that BNP, glyNT-BNP and nonglyNT-BNP all significantly correlated with LVEF, FS and LVMI to similar degrees (table 5).

Study 3

In our gel filtration HPLC analysis of atrial extracts from patients with HF, we observed two peaks in NT-BNP immunoreactivity (figure 8A). The larger peak corresponded to the elution point of nonglyNT-BNP, while the smaller peak corresponded to the elution point of proBNP-108. After enzymatic deglycosylation, the amplitude of the larger peak was nearly doubled, suggesting that glyNT-BNP and nonglyNT-BNP were present at similar concentrations in the atrial tissue. In contrast, there was no remarkable change in the other peak. Two peaks of BNP immunoreactivity were also observed. The larger peak corresponded to BNP-32, while the smaller peak corresponded to proBNP-108. The molar ratio of BNP to nonglyNT-BNP before the enzymatic deglycosylation procedure was 1:0.76, while the molar ratio of BNP to total NT-BNP after deglycosylation was 1:1.42. Deglycosylation had no effect on the BNP peaks. In atrial tissue, the cross-reactivity of NT-BNP with proBNP-108 was 11±3% before deglycosylation. Consistent with the gel filtration HPLC analysis, we found that the atrial concentrations of BNP, nonglyNT-BNP and glyNT-BNP were comparable (figure 8B).

The relationships between glyNT-BNP and nonglyNT-BNP and BNP in atrial tissue are shown in figure 8C,D, respectively. Atrial glyNT-BNP levels closely correlated with the levels of nonglyNT-BNP and BNP (nonglyNT-BNP, $r=0.611$; BNP, $r=0.829$; all $p<0.01$) (figure 8C,D). In addition, the nonglyNT-BNP levels also significantly correlated with the BNP levels ($r=0.749$, all $p<0.0001$, figure 8E).

DISCUSSION

Within the heart, proBNP-108 is normally cleaved to form BNP-32 and NT-BNP, which are then secreted into the circulation,[1–4]

but recent studies have shown that levels of unprocessed proBNP-108 are increased in HF.[15 16] Moreover, the proBNP-108 to BNP-32 ratio is increased to a greater degree in HF with ventricular overload than with atrial overload.[10] In addition, proBNP-108 is *O*-glycosylated at seven sites in the N-terminal portion of the peptide,[5–7] which suggests that a significant amount of glyNT-BNP is circulating in the plasma of patients with HF or CRF, though up to now the levels of glyNT-BNP in patients with HF and patients with CRF on haemodialysis were unknown. In the present study, we measured immunoreactive NT-BNP levels in the plasma of these patients using the Elecsys proBNP I, with and without enzymatic deglycosylation. The signal antibody in this assay system recognises the midportion of NT-BNP, but the *O*-linked oligosaccharide attachments at amino acids 44 and 48 almost completely blocked the binding of this antibody (figure 1).[5 7] Our observation that plasma NT-BNP levels appeared to increase for 16–24 h during enzymatic deglycosylation until finally reaching a plateau indicates that NT-BNP was completely deglycosylated at that point.

Atrial molar levels of BNP and total NT-BNP were similar, suggesting that BNP and total NT-BNP are secreted from the heart in equimolar fashion. In contrast, nonglyNT-BNP levels were 2.5 times higher than the BNP levels in plasma from patients with HF, which is consistent with earlier reports.[17 18] Plasma BNP is cleared from the blood via several pathways, including binding to natriuretic peptide receptors-A and -C, excretion in the urine, and metabolism by neutral enzymes and/or unknown proteases in the blood. In contrast, clearance of nonglyNT-BNP largely depends on renal excretion.[19] As a result, nonglyNT-BNP has a longer half-life in blood than BNP (~120 min vs 20 min),[3] which probably contributes to the higher plasma nonglyNT-BNP levels.

In the present study, we initially found that plasma glyNT-BNP was four times higher than nonglyNT-BNP in patients with HF, and that glyNT-BNP levels increased in proportion to disease severity, as was also seen with nonglyNT-BNP and BNP. In addition, the molar ratio of nonglyNT-BNP to glyNT-BNP in plasma was constant and independent of HF severity, suggesting that the half-life of glyNT-BNP in blood is longer than that of nonglyNT-BNP. Post-translational modifications play an important role in protein biosynthesis, stability and biological activity, and glycosylation is one of the most common and diverse post-translational modifications.[20 21] Carbohydrate moieties in proteins are known to be important for normal cellular function, enzyme activity and protein–protein interactions.[20–22] A recent study by Jiang *et al*[23] showed that proBNP contains a substantial number of *O*-glycans, which are terminally sialylated. In addition, they showed that the *O*-glycan inhibitor Ben-gal shortened the half-life of proBNP in the medium of HEK-293 and HL-1 cells.[23] We observed that plasma levels of glyNT-BNP were higher than those of nonglyNT-BNP, although the levels were similar in atrial lysates, which is in good agreement with the findings of Jiang *et al*. Thus, attachment of *O*-glycans to NT-BNP may increase its resistance to clearance from the blood.

Previous studies showed that plasma nonglyNT-BNP levels are increased in proportion to the reduction of estimated glomerular filtration.[24 25] We also observed that nonglyNT-BNP levels were ~20 times higher than the BNP levels in patients with CRF on haemodialysis, which is consistent with earlier findings.[26 27] Moreover, glyNT-BNP levels were ~10 times higher than the nonglyNT-BNP levels in those patients and, in contrast to other peptides and substances,[28] glyNT-BNP levels did not decline after haemodialysis. Consequently, the percentage glycosylation increased after haemodialysis to >90%, suggesting that >90% of total NT-BNP is invisible to the assay and therefore underestimated. Although the exact mechanism underlying the accumulation of glyNT-BNP in patients with CRF on haemodialysis remains unknown, we would speculate that attachment of *O*-glycans to NT-BNP probably inhibits its removal during haemodialysis.

The clinical utility of measuring the extremely elevated glyNT-BNP remains unknown, at present. BNP and nonglyNT-BNP have been used as markers of cardiac function for diagnosing HF, and as prognostic indicators of cardiovascular disease, even in patients with CRF on haemodialysis.[26 29 30] Indeed, in the present study, plasma BNP levels correlated significantly with cardiac function (FS and LVEF) and left ventricular mass (LVMI), which is consistent with earlier findings. In addition, we found that cardiac function and structure correlated similarly with glyNT-BNP and nonglyNT-BNP, which suggests that glyNT-BNP may be as useful a marker of cardiac function and/or left ventricular mass as BNP or nonglyNT-BNP.

We observed modest correlations between cGMP and ANP and BNP in CRF, but a weaker correlation between cGMP and glyNT-BNP (figure 7). Although BNP and glyNT-BNP are encoded by the same gene, their behaviour and metabolism in blood differ somewhat. Plasma levels of glyNT-BNP change more slowly than BNP levels due to its longer half-life, and its molar levels are 80 times higher than those of BNP in patients with CRF on haemodialysis. These pharmacodynamics suggest that accumulation of glyNT-BNP in patients with CRF on haemodialysis reflects the integrated wall stress in the heart, rather than momentary stress. This raises the possibility that glyNT-BNP would be a better prognostic marker than BNP or nonglyNT-BNP in HF and/or CRF, but that remains to be tested.

Taken together, we found that plasma levels of undetectable glyNT-BNP are increased in patients with HF and patients with CRF on haemodialysis. This remarkable increase in glyNT-BNP is likely to be caused by diminished metabolism. A schematic diagram depicting a model of the production, secretion and metabolism of nonglyNT-BNP, glyNT-BNP and BNP suggested by our findings is shown in figure 9. Whether glyNT-BNP levels are a better marker than BNP or nonglyNT-BNP for diagnosis and more predictive of prognosis in HF and CRF will be determined in future studies.

Acknowledgements We thank Ms Masako Minato, Ms Kyoko Tabei, Ms Keiko Fukuda, Mr Kazumi Akimoto and Ms Machiko Sakata for their technical assistance with measuring BNP, nonglyNT-BNP and glyNT-BNP. We thank Mr Yoshibumi Akutsu for his technical assistance with the echocardiography. We also thank Dr Naoto Minamino for helpful advice.

Funding This study was supported in part by Scientific Research Grants-in-Aid 18590787 and 20590837 from the Ministry of Education, Culture, Sports, Science and Technology of Japan and by the Science Research Promotion Fund from the Promotion and Mutual Aid Corporation for Private Schools of Japan.

Competing interests None.

Ethics approval Ethics approval was provided by the ethics committee of the authors' institute and was carried out in accordance with the recommendations of the ethical committee of Dokkyo Medical University.

Contributors TN designed the study, analysed the results and wrote the manuscript. MI contributed the gel filtration analysis. YT and TI analysed the results of heart failure. IS and HF contributed the study of atrial tissue analysis of BNP and NY-BNP. HK, NY and KK measured NT-BNP with and without the enzyme cocktail. KK is the supervisor and provided useful comments on the manuscript.

Provenance and peer review Not commissioned; externally peer reviewed.

REFERENCES

1. **Nishikimi T,** Kuwahara K, Nakao K. Current biochemistry, molecular biology, and clinical relevance of natriuretic peptides. *J Cardiol* 2011;**57**:131–40.

2. **Nishikimi T,** Maeda N, Matsuoka H. The role of natriuretic peptides in cardioprotection. *Cardiovasc Res* 2006;**69**:318—28.
3. **Weber M,** Hamm C. Role of B-type natriuretic peptide (BNP) and NT-proBNP in clinical routine. *Heart* 2006;**92**:843—9.
4. **Daniels LB,** Maisel AS. Natriuretic peptides. *J Am Coll Cardiol* 2007;**50**:2357—68.
5. **Schellenberger U,** O'Rear J, Guzzetta A, *et al*. The precursor to B-type natriuretic peptide is an O-linked glycoprotein. *Arch Biochem Biophys* 2006;**451**:160—6.
6. **Liang F,** O'Rear J, Schellenberger U, *et al*. Evidence for functional heterogeneity of circulating B-type natriuretic peptide. *J Am Coll Cardiol* 2007;**49**:1071—8.
7. **Seferian KR,** Tamm NN, Semenov AG, *et al*. Immunodetection of glycosylated NT-proBNP circulating in human blood. *Clin Chem* 2008;**54**:866—73.
8. **Luckenbill KN,** Christenson RH, Jaffe AS, *et al*. Cross-reactivity of BNP, NT-proBNP, and proBNP in commercial BNP and NT-proBNP assays: preliminary observations from the IFCC Committee for Standardization of Markers of Cardiac Damage. *Clin Chem* 2008;**54**:619—21.
9. **Hammerer-Lercher A,** Halfinger B, Sarg B, *et al*. Analysis of circulating forms of proBNP and NT-proBNP in patients with severe heart failure. *Clin Chem* 2008;**54**:858—65.
10. **Nishikimi T,** Minamino N, Ikeda M, *et al*. Diversity of molecular forms of plasma brain natriuretic peptide in heart failure—different proBNP-108 to BNP-32 ratios in atrial and ventricular overload. *Heart* 2010;**96**:432—9.
11. **Nishikimi T,** Saito Y, Kitamura K, *et al*. Increased plasma levels of adrenomedullin in patients with heart failure. *J Am Coll Cardiol* 1995;**26**:1424—31.
12. **Nishikimi T,** Karasawa T, Inaba C, *et al*. Effects of long-term intravenous administration of adrenomedullin (AM) plus hANP therapy in acute decompensated heart failure: a pilot study. *Circ J* 2009;**73**:892—8.
13. **Yoshitomi Y,** Nishikimi T, Abe H, *et al*. Comparison of changes in cardiac structure after treatment in secondary hypertension. *Hypertension* 1996;**27**:319—23.
14. **Quiones GA,** Douglas PS, Foster E, *et al*. ACC/AHA clinical competence statement on echocardiography: a report of the American College of Cardiology/ American Heart Association/American College of Physicians-American Society of Internal Medicine Task Force on Clinical Competence. Developed in collaboration with the American Society of Echocardiography, the Society of Cardiovascular Anesthesiologists, and the Society of Pediatric Echocardiography. *J Am Coll Cardiol* 2003;**41**:687—708.
15. **Waldo SW,** Beede J, Isakson S, *et al*. Pro-B-type natriuretic peptide levels in acute decompensated heart failure. *J Am Coll Cardiol* 2008;**51**:1874—82.
16. **Xu-Cai YO,** Wu Q. Molecular forms of natriuretic peptides in heart failure and their implications. *Heart* 2010;**96**:419—24.
17. **Vickery S,** Price CP, John RI, *et al*. B-type natriuretic peptide (BNP) and amino-terminal proBNP in patients with CKD: relationship to renal function and left ventricular hypertrophy. *Am J Kidney Dis* 2005;**46**:610—20.
18. **Sakai H,** Tsutamoto T, Ishikawa C, *et al*. Direct comparison of brain natriuretic peptide (BNP) and N-terminal pro-BNP secretion and extent of coronary artery stenosis in patients with stable coronary artery disease. *Circ J* 2007;**71**:499—505.
19. **Spanaus KS,** Kronenberg F, Ritz E, *et al*; Mild-to-Moderate Kidney Disease Study Group. B-type natriuretic peptide concentrations predict the progression of nondiabetic chronic kidney disease: the Mild-to-Moderate Kidney Disease Study. *Clin Chem* 2007;**53**:1264—72.
20. **Eklund EA,** Freeze HH. Essentials of glycosylation. *Semin Pediatr Neurol* 2005;**12**:134—43.
21. **Varki A.** Biological roles of oligosaccharides: all of the theories are correct. *Glycobiology* 1993;**3**:97—130.
22. **Zachara NE,** Hart GW. The emerging significance of *O*-GlcNAc in cellular regulation. *Chem Rev* 2002;**102**:431—8.
23. **Jiang J,** Pristera N, Wang W, *et al*. Effect of sialylated *O*-glycans in pro-brain natriuretic peptide stability. *Clin Chem* 2010;**56**:959—66.
24. **deFilippi CR,** Seliger SL, Maynard S, *et al*. Impact of renal disease on natriuretic peptide testing for diagnosing decompensated heart failure and predicting mortality. *Clin Chem* 2007;**53**:1511—19.
25. **Schou M,** Alehagen U, Goetze JP, *et al*. Effect of estimated glomerular filtration rate on plasma concentrations of B-type natriuretic peptides measured with multiple immunoassays in elderly individuals. *Heart* 2009;**95**:1514—19.
26. **Bargnoux AS,** Klouche K, Fareh J, *et al*. Prohormone brain natriuretic peptide (proBNP), BNP and N-terminal-proBNP circulating levels in chronic hemodialysis patients. Correlation with ventricular function, fluid removal and effect of hemodiafiltration. *Clin Chem Lab Med* 2008;**46**:1019—24.
27. **Racek J,** Krlov H, Trefil L, *et al*. Brain natriuretic peptide and N-terminal proBNP in chronic haemodialysis patients. *Nephron Clin Pract* 2006;**103**:162—72.
28. **Wahl HG,** Graf S, Renz H, *et al*. Elimination of the cardiac natriuretic peptides B-type natriuretic peptide (BNP) and N-terminal proBNP by hemodialysis. *Clin Chem* 2004;**50**:1071—4.
29. **Nishikimi T,** Futoo Y, Tamano K, *et al*. Plasma brain natriuretic peptide levels in chronic hemodialysis patients: influence of coronary artery disease. *Am J Kidney Dis* 2001;**37**:1201—8.
30. **Frankenstein L,** Clark AL, Goode K, *et al*. The prognostic value of individual NT-proBNP values in chronic heart failure does not change with advancing age. *Heart* 2009;**95**:825—9.

J Pharmacol Sci 116, 337 – 342 (2011)

Journal of Pharmacological Sciences

Forum Minireview

New Molecular Mechanisms for Cardiovascular Disease: Transcriptional Pathways and Novel Therapeutic Targets in Heart Failure

Koichiro Kuwahara[1,*] and Kazuwa Nakao[1]

[1]*Department of Medicine and Clinical Science, Kyoto University Graduate School of Medicine, Kyoto 606-8507, Japan*

Received October 21, 2010; Accepted November 8, 2010

Abstract. Genetic remodeling contributes to the progression of heart failure by affecting myocardial cellular function and survival. In our investigation of the transcriptional regulation of cardiac gene expression, we found several transcriptional pathways involved in pathological cardiac remodeling. A transcriptional repressor, neuron-restrictive silencer factor (NRSF), regulates expression of multiple fetal cardiac genes through the activity of histone deacetylases (HDACs). Inhibition of NRSF in the heart results in cardiac dysfunction and sudden arrhythmic death accompanied by re-expression of a number of fetal genes, including those encoding fetal ion channels, such as the T-type Ca^{2+} channel. In the pathological calcineurin – nuclear factor of activated T-cells (NFAT) signaling pathway, transient receptor potential cation channel, subfamily C, member 6 (TRPC6) is a key component of a Ca^{2+}-dependent regulatory loop. Indeed, inhibition of TRPC significantly ameliorates this pathological process in a mouse model of cardiac hypertrophy. Moreover, we recently showed that myocardin-related transcription factor-A (MRTF-A), a co-activator of serum response factor (SRF), mediates prohypertrophic signaling by linking the small GTPase Rho-actin dynamics signaling pathway to cardiac gene transcription. Collectively, our studies have revealed the transcriptional network involved in the development of cardiac dysfunction and potential therapeutic targets for the treatment of heart failure.

Keywords: neuron-restrictive silencer factor (NRSF), myocardin-related transcription factor-A (MRTF-A), transient receptor potential cation channel, heart failure, cardiovascular disease

1. Introduction

In response to pathological stimuli such as prolonged mechanical stress or abnormal neurohumoral activation, hearts show hypertrophic growth and remodeling characterized by an increase in myocyte cell size, assembly of sarcomere proteins, interstitial fibrosis, and re-expression of fetal cardiac genes. Although the hypertrophic response is initially compensatory, it ultimately leads to heart failure, which is now a leading cause of morbidity and mortality around the world. Diverse intracellular signaling pathways, which ultimately affect nuclear factors and the regulation of gene expression, have been shown to play important roles in the pathological processes involved in cardiac remodeling (1). Unraveling the details of these pathways should give us a better understanding of the molecular processes underlying the establishment of cardiac hypertrophy and heart failure and could ultimately lead to the discovery of novel therapeutic targets for the prevention of pathological cardiac remodeling and heart failure. In this review, we introduce our recent findings regarding the signal transduction cascades that drive transcriptional remodeling during the pathological process of heart failure.

*Corresponding author. kuwa@kuhp.kyoto-u.ac.jp
Published online in J-STAGE on July 14, 2011 (in advance)
doi: 10.1254/jphs.10R28FM

2. NRSF-HDAC repressor complex regulates multiple fetal cardiac genes

Neuron-restrictive silencer element (NRSE), also known as repressor element 1 (RE-1), was originally

identified as a negative-acting DNA regulatory element that prevents expression of neuronal genes in non-neuronal cell types and in undifferentiated neuronal cells (2, 3). A transcriptional repressor, neuron-restrictive silencer factor (NRSF), also known as RE-1 silencing transcription factor (REST), binds to NRSE to exert its regulatory effects (4, 5). We reported that NRSE is present within the transcriptional regulatory region of multiple fetal cardiac genes, such as those encoding ANP, BNP, skeletal α-actin, and fetal ion channels, and that it plays a pivotal role in the regulation of the expression of these genes in cardiac myocytes (6 – 8). The NRSE–NRSF system represses fetal cardiac gene expression in ventricular myocytes by recruiting the class I histone deacetylases (HDACs) HDAC-1 and -2, and the class II HDACs HDAC-4 and -5 (9). Whereas class I HDACs are expressed relatively ubiquitously, class II HDACs, which include HDAC-4, -5, -7, and -9, are expressed in a tissue-specific manner, with highest expression in heart, brain, and skeletal muscle, where they reportedly act as signal-responsive repressors of cardiac hypertrophy (10). Hypertrophic stimulus–induced phosphorylation of two conserved phosphorylation sites by calcium/calmodulin kinase (CaMK) causes class II HDACs to be exported from the nucleus, resulting in derepression of their target genes. In other words, nuclear export of class II HDACs induced by hypertrophic stimuli attenuates NRSF-mediated repression, thereby activating the fetal gene program in cardiac myocytes (Fig. 1) (9).

Transgenic mice expressing a dominant-negative NRSF mutant in their hearts exhibit dilated cardiomyopathy and sudden arrhythmic death, suggesting the NRSF–HDAC repressor complex plays a key role in the molecular pathways underlying the progression of heart failure and sudden death (8). In dnNRSF-Tg hearts, expression of *CACNA1H*, which encodes the T-type Ca^{2+} channel α subunit, was increased. Moreover, T-type Ca^{2+} current ($I_{ca,T}$) amplitude was correspondingly increased in ventricular myocytes isolated from dnNRSF-Tg hearts, suggesting $I_{ca,T}$ in some way contributes to the susceptibility of dnNRSF-Tg hearts to arrhythmias (8). Consistent with this notion, efonidipine and mibefradil, dual T- and L-type Ca^{2+} channel blockers, but not nitrendipine, a more L-type–selective Ca^{2+}-channel blocker, significantly improved the survival and arrhythmogenicity in dnNRSF-Tg mice (11). The *R*(−)-isomer of efonidipine [*R*(−)-efonidipine], a recently identified, highly selective T-type Ca^{2+}- channel blocker, also substantially prolonged the survival of dnNRSF-Tg mice (11, 12). In addition, efonidipine prevented the deaths of mice with myocardial infarction, whereas nitrendipine did not. These findings demonstrate that T-type Ca^{2+}-channel blockade may represent a new and effective means of preventing sudden cardiac death in patients with heart failure.

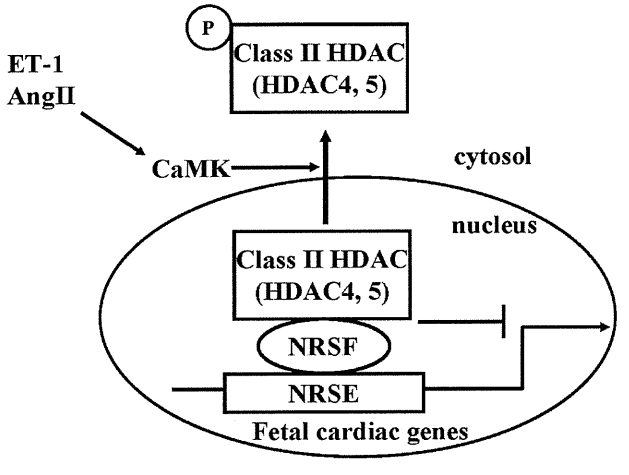

Fig. 1. The NRSF-HDACs repressor complex regulates the expression of multiple fetal cardiac genes. ET-1: endothelin-1, AngII: angiotensin II, CaMK: calcium/calmodulin kinase, HDAC: histone deacetylase.

3. TRPC6 is a nodal point for pro- and anti-hypertrophic signaling

The serine-threonine phosphatase calcineurin (PP2B) functions as a Ca^{2+}-dependent regulator of cardiac hypertrophy and the fetal gene program (13). Calcineurin dephosphorylates nuclear factor of activated T-cells (NFAT) family transcription factors and induces their translocation to the nucleus, where they bind to the regulatory regions of cardiac genes in conjunction with other cardiac transcription factors and promote hypertrophic growth (13). Sustained entry of Ca^{2+} across the plasma membrane via agonist- or receptor-activated Ca^{2+}-entry channels is thought to contribute to the activation of the calcineurin–NFAT pathway, but many of the details of the mechanisms involved in these processes remain to be elucidated. Receptor-activated Ca^{2+} entry is initiated upon the binding of hormones or growth factors to G-protein–coupled receptors or receptor tyrosine kinases, leading to activation of phospholipase C (PLC) and subsequent cleavage of phosphatidylinositol 4,5-biphosphate (PIP2) into diacylglycerol (DAG) and inositol-1,4,5-trisphosphate (IP3) (14, 15). Recent evidence indicates that transient receptor potential (TRP) proteins are likely channel subunits responsible for receptor-activated Ca^{2+} entry (14, 16). Initially identified in *Drosophila* (16) as receptor-activated cation channels (*Drosophila* TRP and TRP-like), 28 mammalian TRP-channel homologues have been identified to date. The mammalian TRP family

has been further classified into seven subfamilies based on their structures, including canonical TRP (TRPC), vanilloid TRP (TRPV), melastatin TRP (TRPM), TRPN, TRPP, TRPML, and TRPA (14). Structurally, the seven members of the TRPC subfamily are the most closely related to *Drosophila* TRP (14). Among the TRPC channels, TRPC-3, -6 and -7 are 75% identical and gated via signal transduction pathways that activate PLC, as well as by direct exposure to DAG (17). Thus, TRPC-3, -6, and -7 form a subfamily of second-messenger–operated cation channels coupling receptor-PLC signaling pathways to Ca^{2+} entry (14).

The involvement of TRPC channels in cardiac calcineurin–NFAT signaling was examined, and it was found that expression of TRPC6 mRNA is specifically up-regulated in the hearts of mice expressing constitutively active calcineurin and subjected to pressure overload caused by transverse aortic banding (18). The 5′-flanking region of the *TRPC6* gene contains two conserved NFAT-binding sites that confer responsiveness to calcineurin–NFAT signaling. Cardiac-specific overexpression of TRPC6 in transgenic mice resulted in cardiomyopathy with a pronounced increase in the expression of β-MHC, a sensitive marker for pathological hypertrophy. Similarly, overexpression of TRPC6 in cardiomyocytes activated the NFAT-dependent promoter of the *Regulator of Calcineurin 1 (RCAN1)* gene and siRNA knockdown of TRPC6 reduced hypertrophic signaling by phenylephrine and endothelin-1, suggesting that TRPC6 is involved in G-protein–coupled receptor-dependent activation of the calcineurin–NFAT pathway. These findings demonstrate that TRPC6 completes a positive regulatory circuit for calcineurin–NFAT signaling during pathological cardiac remodeling and activation of fetal cardiac gene expression (Fig. 2) (18).

Characterization of the cross-talk among the cardiac signaling pathways that promote or antagonize hypertrophic responses should lead to a better understanding of the molecular processes underlying the establishment of cardiac hypertrophy and heart failure. We therefore investigated the signaling pathways that negatively regulate the TRPC6–calcineurin–NFAT pathway. It was recently shown that the activities of TRPC-3 and -6 are greatly attenuated by cGMP-protein kinase G (PKG)–catalyzed phosphorylation of Thr11 and Ser263 in TRPC3 and Thr69 in TRPC6, which are well conserved among mouse, rat, and human (19, 20). We studied the functionally negative cross-talk between the antihypertrophic atrial and brain natriuretic peptide (ANP and BNP, respectively) – guanylyl cyclase-A (GC-A) – PKG pathway and the prohypertrophic TRPC6–calcineurin–NFAT pathway during the process of cardiac hypertrophy, and characterized its biological significance in cardiac

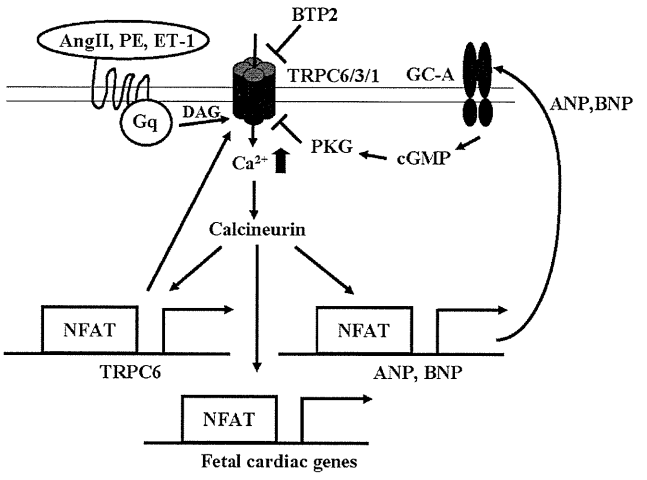

Fig. 2. TRPC6 contributes to the augmentation of pathological calcineurin–NFAT signaling, whereas ANP/BNP – GC-A signaling inhibits this pathway by blocking TRPC6 activity via PKG in cardiac myocytes. PE: phenylephrine.

pathophysiology. We found that TRPC6 is phosphorylated at Thr69 via the ANP/BNP – GC-A – PKG antihypertrophic signaling pathway, which strongly attenuated TRPC6 activity. Cardiac hypertrophy was also significantly attenuated by the selective TRPC inhibitor BTP2 in GC-A knockout (KO) mice, which were hypersensitive to hypertrophic signaling caused by overexpression of TRPC6. Likewise, BTP-2 significantly inhibited the cardiac hypertrophy induced by chronic angiotensin II infusion. Thus inhibition of TRPC6 activity contributes to the antihypertrophic effects of ANP/BNP, which suggests inhibition of TRPC6 could be an effective therapeutic strategy for preventing pathological cardiac hypertrophy and remodeling (Fig. 2) (21).

It has been shown in separate studies that GC-A is desensitized in failing human hearts (22) and that angiotensin II and endothelin-1 act to desensitize GC-A (23). This makes it unlikely that, under pathological conditions, endogenous cardiac ANP/BNP – GC-A – PKG signaling would be sufficient to block the pathological signaling activity. Such disruption of the balance between anti- and pro-hypertrophic signaling would lead to further activation of TRPC3/6-dependent pro-hypertrophic signaling, thereby promoting pathological cardiac remodeling. Thus inhibition of TRPC3/6 channel activity could be an effective therapeutic strategy for preventing cardiac remodeling under these conditions. Indeed, our finding that BTP2 attenuated cardiac hypertrophy in GC-A KO and angiotensin II–infused mice may support this notion. Development of highly specific TRPC6 inhibitors could lead to the production of more potent and safer agents with which to prevent pathological cardiac remodeling

and heart failure.

4. MRTF-A is a novel transcriptional mediator linking actin remodeling and cardiac gene expression

Hemodynamic overload caused by a combination of mechanical stress and neurohumoral stimulation induces a hypertrophic response characterized in part by reactivation of the fetal gene program in cardiac myocytes (1, 24). Among the variety of intracellular signaling molecules known to be activated following mechanical stretch or neurohumoral stimulation, Rho family small GTPases, especially Rho A and Rac1, have been highlighted as important regulators for cardiac hypertrophy (25, 26).

A transcriptional activator, serum response factor (SRF), has been shown to be involved in the downstream mechanisms by which Rho GTPases activate the hypertrophic gene program. SRF is a MADS-box transcription factor that regulates the expression of immediate early genes and muscle-specific genes by binding to a conserved sequence [CC (A/T) $_6$GG] known as the CArG box or serum response element. In this way, SRF plays an important role in the induction of a subset of cardiac genes during adverse cardiac remodeling. Targeted deletion of SRF in the developing heart results in lethal cardiac defects with reduced expression of many cardiac-specific genes (27, 28). In addition, overexpression of SRF in the postnatal heart leads to cardiomyopathy with increased fetal cardiac gene expression (29), while conditional deletion of SRF in isolated neonatal cardiac myocytes results in reduced expression of hypertrophic genes (30). Indeed, several fetal cardiac genes, including ANP, skeletal α-actin, smooth muscle α-actin, and smooth muscle 22α, contain a functionally important CArG box in their upstream transcription control regions (31, 32). At least two signaling pathways are known to modulate SRF activity: one involving the phosphorylation of ternary complex factors in Ets-domain family proteins and another controlled by Rho-family small GTPases and actin dynamics (33, 34). It was recently shown in NIH3T3 cells that stimulation of Rho- and actin dynamics–dependent signaling results in translocation of a novel SRF co-factor, myocardin-related transcription factor (MRTF)-A (also known as MAL or MKL1), from G-actin in the cytoplasm to the nucleus, leading to activation of SRF target genes (35, 36).

We further showed that Rho- and actin treadmill–dependent nuclear accumulation of MRTF-A contributes to the transduction of mechanical stress to SRF-dependent transcriptional activation of fetal cardiac genes in cardiac myocytes. In mice lacking MRTF-A, induction of BNP and other fetal cardiac genes in response to both acute and chronic pressure overload was significantly attenuated. We also revealed the involvement of MRTF-A in chronic cardiac remodeling, a process in which neurohumoral factors play a pivotal role. Following stimulation with angiotensin II or endothelin-1, MRTF-A was translocated into the nuclei of cardiac myocytes, where it activated SRF. Moreover, MRTF-A$^{-/-}$ mice showed significantly weaker hypertrophic responses than their wild-type littermates. Collectively, these findings indicate that MRTF-A is a common mediator of mechanical stress– and neurohumoral stimulation–induced prohypertrophic signaling (Fig. 3) (37).

The inhibition of Rho or ROCK (Rho kinase), a downstream target of Rho, ameliorates pathological cardiac hypertrophy (25, 38, 39). Our study defines MRTF-A as a critical downstream mediator of Rho- and actin dynamics–associated prohypertrophic signaling in cardiac myocytes, while others have shown that in epithelial cells MRTF-A is also activated downstream of Rac (40). Two important events that occur downstream of Rho and Rac activation are alteration of actin cytoskeletal organization and gene transcription, and MRTF-A is a key mediator of the latter. Consequently, diminishing MRTF-A–mediated transcriptional activation by inhibiting its nuclear translocation and/or its co-activator function, which would selectively block transcriptional pathways activated downstream of Rho family small GTPases, could be a safer and more specific therapeutic approach to preventing pathological cardiac remodeling, without the potential side effects caused by disruption of the physiological organization of the actin-cytoskeleton (Fig. 3).

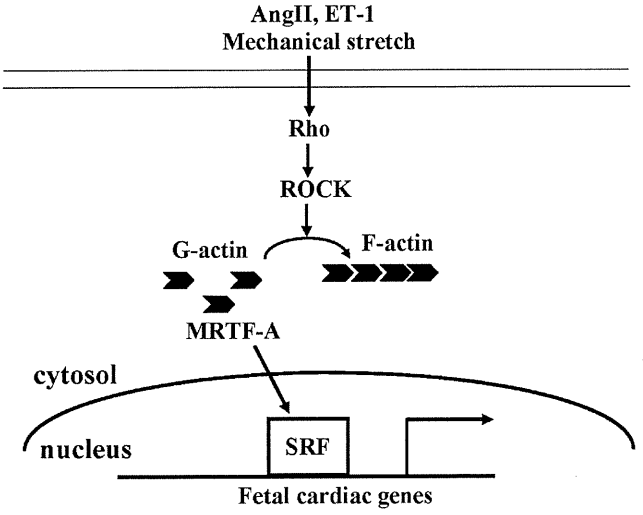

Fig. 3. Nuclear translocation of MRTF-A following Rho–ROCK activation and actin remodeling mediates both mechanical stress– and neurohumoral stimulation–inducible hypertrophic gene reprogramming.

5. Conclusion

Genetic remodeling contributes to the progression of heart failure by affecting myocardial cellular function and survival. Exploring the transcriptional pathways involved in pathological cardiac remodeling will lead to a better understanding of the molecular mechanisms underlying the development of pathological processes in the heart and will ultimately provide us with an opportunity to shed light on new molecular effectors with the potential to have a therapeutic impact on human heart failure. In this mini-review, we have introduced our work on the transcriptional pathways involved in pathological cardiac remodeling. A transcriptional repressor, NRSF, represses expression of multiple fetal cardiac genes through recruitment of HDACs, and attenuation of this NRSF-mediated repression appears to contribute to the re-expression of fetal cardiac genes in diseased hearts. Inhibition of NRSF in the heart results in cardiac dysfunction and sudden arrhythmic death accompanied by re-expression of multiple fetal genes, including those encoding fetal ion channels, such as the T-type Ca^{2+} channel. Conversely, T-type Ca^{2+}-channel blockade significantly prolongs survival in dnNRSF-Tg mice (12). TRPC6 is a key integrated component of the calcineurin–NFAT signaling circuit, and its inhibition significantly ameliorates the pathological process in mouse models of cardiac hypertrophy. This at least in part reflects the fact that inhibition of TRPC6 contributes to the antihypertrophic effects exerted by ANP/BNP – GC-A – PKG signaling, which suggests TRPC6 blockade could be a novel therapeutic strategy for preventing pathological cardiac remodeling. Finally, we revealed a new signaling mechanism whereby MRTF-A, a co-activator of SRF, mediates both mechanical stress– and neurohumoral stimulation–induced prohypertrophic signaling by linking the small GTPase Rho-actin dynamics signaling pathway to cardiac gene transcription. Collectively, our studies on the transcriptional network underlying the pathological cardiac remodeling have revealed several potential therapeutic targets; T-type Ca^{2+} channel, TRPC6 channel, and MRTF-A. We anticipate that further study of the transcriptional network involved in the development of cardiac dysfunction will lead to the discovery of new therapeutic targets for the treatment of heart failure.

Acknowledgments

We thank Dr. T. Iwamoto (Fukuoka University) for giving us the opportunity to write this review article. We also thank Y. Kubo for her excellent secretarial work. Work carried in our laboratories is supported by Grants-in-Aid for Scientific Research from the Japan Society for the Promotion of Science (to K.K. and N.K.) and grants from the Japanese Ministry of Health, Labour, and Welfare (to N.K.).

References

1 Olson EN. A decade of discoveries in cardiac biology. Nat Med. 2004;10:467–474.
2 Kraner SD, Chong JA, Tsay HJ, Mandel G. Silencing the type II sodium channel gene: A model for neural-specific gene regulation. Neuron. 1992;9:37–44.
3 Mori N, Schoenherr C, Vandenbergh DJ, Anderson DJ. A common silencer element in the SCG10 and type II Na+ channel genes binds a factor present in nonneuronal cells but not in neuronal cells. Neuron. 1992;9:45–54.
4 Chong JA, Tapia-Ramirez J, Kim S, Toledo-Aral JJ, Zheng Y, Boutros MC, et al. REST: A mammalian silencer protein that restricts sodium channel gene expression to neurons. Cell. 1995; 80:949–957.
5 Schoenherr CJ, Anderson DJ. The neuron-restrictive silencer factor (NRSF): A coordinate repressor of multiple neuron-specific genes. Science. 1995;267:1360–1363.
6 Kuwahara K, Saito Y, Ogawa E, Takahashi N, Nakagawa Y, Naruse Y, et al. The neuron-restrictive silencer element-neuron-restrictive silencer factor system regulates basal and endothelin 1-inducible atrial natriuretic peptide gene expression in ventricular myocytes. Mol Cell Biol. 2001;21:2085–2097.
7 Ogawa E, Saito Y, Kuwahara K, Harada M, Miyamoto Y, Hamanaka I, et al. Fibronectin signaling stimulates BNP gene transcription by inhibiting neuron-restrictive silencer element-dependent repression. Cardiovasc Res. 2002;53:451–459.
8 Kuwahara K, Saito Y, Takano M, Arai Y, Yasuno S, Nakagawa Y, et al. NRSF regulates the fetal cardiac gene program and maintains normal cardiac structure and function. EMBO J. 2003;22: 6310–6321.
9 Nakagawa Y, Kuwahara K, Harada M, Takahashi N, Yasuno S, Adachi Y, et al. Class II HDACS mediate CaMK-dependent signaling to NRSF in ventricular myocytes. J Mol Cell Cardiol. 2006;41:1010–1022.
10 McKinsey TA, Zhang CL, Lu J, Olson EN. Signal-dependent nuclear export of a histone deacetylase regulates muscle differentiation. Nature. 2000;408:106–111.
11 Kinoshita H, Kuwahara K, Takano M, Arai Y, Kuwabara Y, Yasuno S, et al. T-type Ca2+ channel blockade prevents sudden death in mice with heart failure. Circulation. 2009;120:743–752.
12 Furukawa T, Miura R, Honda M, Kamiya N, Mori Y, Takeshita S, et al Identification of R(-)-isomer of efonidipine as a selective blocker of T-type Ca2+ channels. Br J Pharmacol. 2004;143: 1050–1057.
13 Molkentin JD, Lu JR, Antos CL, Markham B, Richardson J, Robbins J, et al. A calcineurin-dependent transcriptional pathway for cardiac hypertrophy. Cell. 1998;93:215–228.
14 Hofmann T, Schaefer M, Schultz G, Gudermann T. Transient receptor potential channels as molecular substrates of receptor-mediated cation entry. J Mol Med. 2000;78:14–25.
15 Montell C. The TRP superfamily of cation channels. Sci STKE. 2005;2005:re3.
16 Minke B, Cook B. TRP channel proteins and signal transduction. Physiol Rev. 2002;82:429–472.
17 Hofmann T, Obukhov AG, Schaefer M, Harteneck C, Gudermann T, Schultz G. Direct activation of human TRPC6 andTRPC3 channels by diacylglycerol. Nature. 1999;397:259–263.
18 Kuwahara K, Wang Y, McAnally J, Richardson JA, Bassel-Duby R, Hill JA, et al. TRPC6 fulfills a calcineurin signaling circuit